EXAMENSARBETE I GEOLOGI VID LUNDS UNIVERSITET

Berggrundsgeologi

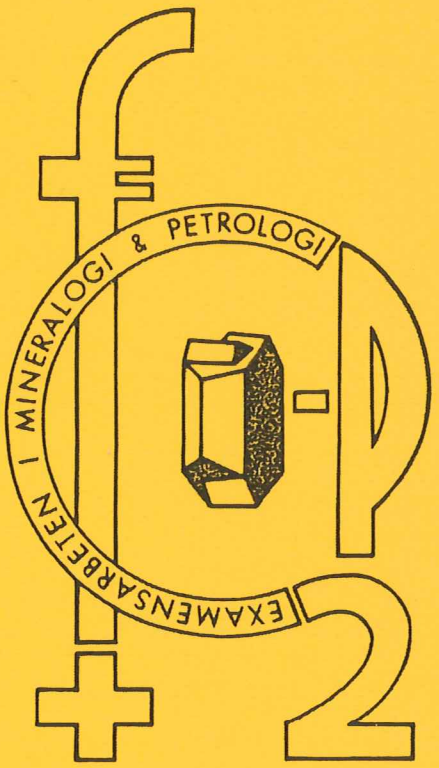

Petrological study of the metamafic rocks across the Småland-Blekinge Deformation Zone

Andrius Rimša

Examensarbete, 20 p
ka Institutionen, Lunds Universitet
Nr 154

CODEN: SE-LUNBDS/NBGO-02/5154+51S

EXAMENSARBETE I GEOLOGI VID LUNDS UNIVERSITET

Berggrundsgeologi

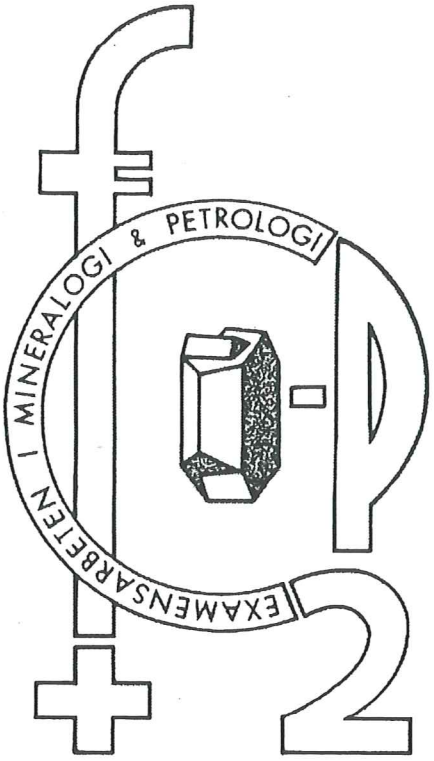

Petrological study of the metamafic rocks across the Småland-Blekinge Deformation Zone

Andrius Rimša

Lund 2002 Examensarbete, 20 p Nr 154
Geologiska Institutionen, Lunds Universitet

Abstract

Petrological study of the metamafic rocks across the Småland-Blekinge Deformation Zone

ANDRIUS RIMŠA

Rimša, A., 2002, Petrological study of the metamafic rocks across the Småland-Blekinge Deformation Zone: Master degree thesis in Geology at Lund University, Dept. of Geology, Nr.154, 51 pp.

The Blekinge-Bornholm province (BBP), in the south- eastern part of Blekinge, consists of foliated granite, granodiorite and tonalite, collectively called the Tving granitoids. The most important tectonic feature in the area is the Småland-Blekinge Deformation Zone (SBDZ). This approximately E-W trending zone separates the TIB Småland-type granitoids in the north from the Tving granitoids in the south. This work focuses on petrological and geochemical comparison of the minor mafic rock bodies occurring mostly within the granitoids on both sides of the SBDZ.

The majority of the metamorphosed, fine-grained mafic rocks (hereafter called "metamafic rocks") to the north of the SBDZ is strictly calc-alkaline, having basalt-andesitic or andesitic compositions. To the south of the SBDZ, however, the fine-grained metamafic rocks have a basaltic composition but splits into two subgroups: one belonging to the calc-alkaline series, the other one to the tholeiitic series. The geochemical and isotopic data suggest that all the fine-grained metamafic rocks across the SBDZ belong to the same rock suite. In addition to the fine-grained metamafic rocks, olivine gabbro and metagabbro compose the Rödeby massif. Here, the olivine gabbro is essentially not metamorphosed and not deformed, whereas the metagabbro probably represents intensely deformed and retrograde metamorphosed parts of the olivine-gabbro intrusion. The relationships of these gabbros with the fine-grained metamafic rocks have not been established.

Mingling and localized mixing between the granitoids and the mafic rocks across the SBDZ evidence for identical ages for the metamafic rocks and the Småland and Tving granitoids, i.e. 1770-1800 Ma. Chemical and isotopic data suggest a uniform depleted mantle source for the mafic rocks and support the hypothesis of Kornfält (2000) of a coherent terrane of the mafic magmatism subsequently cut by the SBDZ. However, the major element variation pattern suggests contamination of the mafic melts by a pre-existing crust that was compositionally different on either side of the SBDZ.

The trace-element characteristics of the metamafic rocks are similar to those of mafic rocks in destructive plate margin environments, which supports the hypothesis that the TIB was formed in an Andinotype, convergent-margin environment.

Andrius Rimša, Lund University, Dept. of Geology, Sölvegatan 13, 223 62 Lund, Sweden.
E-mail: Andrius.Rimsa@novell.geol.lu.se

Sammanfattning

Petrologisk undersökning av metamafiska bergarter på bägge sidor om Småland-Blekinge Deformationzonen

ANDRIUS RIMŠA

Rimša, A., 2002, Petrologisk undersökning av metamafiska bergarter på bägge sidor om Småland-Blekinge Deformationzonen: Examensarbeten i Geologi vid Lunds Universitet, avdelning för Geologi, Nr.154, 51pp.

Den viktigaste tektoniska strukturen i Blekinge-Bornholm Provinsen (BBP), i sydost Blekinge, är den s.k. Småland-Blekinge Deformationszonen (SBDZ). Denna zon har en ungefärlig ost-västlig orientering och separerar Smålandsgranitoiderna, tillhörande TIB i norr från Tvingsgranitoider (graniter, granodioriter, tonaliter) i söder. Detta arbete en petrologisk och geokemisk jämnförelse av små mafiska massiv som förekommer i granitoiderna på båda sidor av SBDZ.

Huvuddelen av de finkorniga, metamorfoserade, mafiska bergarterna (i fortsättningen kallade för metamafiska bergarter) norr om SBDZ är strikt kalk-alkalina, vars sammansättning varierar från basalt-andesiter till andesiter. Samtidigt uppvisar de finkristallina metamafiska bergarterna söder om SBDZ en basaltisk sammansättning kan vidare indelas i två grupper: den ena uppvisar en basaltisk sammansättning och tillhör en kalk-alkalin serie, medan den andra tillhör en tholeiitisk serien. Geokemi och isotopdata indikerar att samtliga finkorniga metamafiska bergarter på bägge sidor om SBDZ tillhör samma bergartssvit. Förutom de två förstnämnda grupperna uppträder olivingabbro och metagabbro tillsammans i Rödebymassivet. Olivingabbron i Rödebymassivet är ometamorfoserad och odeformerad, medan metagabbron antas vara en starkt deformerade och retrogradmetamorfoserade delen av intrusionen. Massivets förhållande till de finkorniga, metamafiska bergarterna är inte utrett.

Mingling och lokaliserad mixing mellan granitoiderna och mafiska bergarter på ömse sidor av SBDZ indikerar en liknande ålder för de metamafiska bergarterna som för Smålands- och Tvingsgranitoiderna, nämligen 1770-1800 Ma. Geokemi och isotopdata antyder en enhetligt utarmad mantel som källa för de mafiska bergarterna på ömse sidor av SBDZ och stödjer därmed Kornfälts (2000) hypotes om en sammanhängande terräng vid tiden för av den mafiska magmatismen. Dessutom antyder skillnader i huvudelementkoncentrationen kontaminering av den mafiska smältan med äldre jordskorpematerial av olikartad sammansättning på ömse sidor av SBDZ.

Spårelementfördelningen för de metamafiska bergarterna liknar den för destruktiva plattgränser och ger stöd för tolkningen att TIB bildades längs en konvergerande plattgräns liknande den för Anderna idag.

Andrius Rimša, Lunds Universitet, avdelning för Geologi, Sölvegatan 13, 223 62 Lund, Sverige.
E-post: Andrius.Rimsa@novell.geol.lu.se

Popular science abstract

The eastern part of Blekinge consists of foliated granitic rocks, collectively called the Tving granitoids. The most important tectonic feature in the area is the Småland- Blekinge Deformation Zone (SBDZ). This deformation zone is a result of movements in the Earth's crust along which rocks have been squeezed in. This movement zone indicates that the part of Blekinge that is situated to the south of the SBDZ was uplifted along this zone compared to its northern side.

To the north of this approximately EW-trending zone the Småland-type granitoids appear, which are part of the Transscandinavian Igneous Belt (TIB). The TIB is a 1.85- 1.65 billion years old giant array of granitoids extending for more than 1500 km in N-S direction across Scandinavia. The Tving granitoids appearing to the south of the SBDZ belong to a problematic geological unit, because it is unclear whether they are part of the TIB or if they belong to different geological terrane. I tried to answer this question by comparing small mafic rocks massifs, which appear within the granitoids on both sides of the SBDZ. Field and microscopic observation, together with geochemical models indicate mingling and localized mixing between the granitoids and mafic rocks across the SBDZ. Mafic and granitic magmas have different physical properties, therefore they do not mix and behave like water and oil in the same pot. The mingling is an indicator that granitic and mafic magmas were intruding each other while they were still not totally crystallized, i.e. both rocks are of the same age and originated during the same magmatic event.

The metamorphosed, fine-grained mafic rocks are similar on both sides of the SBDZ. The geochemical data, which are sensitive to preserve the characteristics of the source of the melt, suggest that all the fine-grained mafic rocks across SBDZ were derived from the same source, i.e. formed during the same magmatic event.

Keeping in mind that all the metamafic rocks belong to the same rock suite and have formed during the same igneous event as the granitoids across the SBDZ it is logical to conclude that the eastern Blekinge granitoids should be included into the TIB.

Mafic rocks are formed during melting of the mantle. Certain chemical elements can be used to get a hint in which plate tectonic situation, they, and related granitoids, were formed.

The geochemical data of metamafic rocks across the SBDZ are similar to those in a subduction zone, where one plate is subducting under another like a floe in the ice-drift. The best recent example of such a plate tectonic situation is the western coast of South America, where the Andes mountain chain is still building up due to subduction of the Pacific oceanic plate under the South American continental pate.

If one decides to make an excursion in time and space to experience how Småland and Blekinge looked like 1,8 billion years ago- the Andes are the most recommended location!

CONTENTS:

I. INTRODUCTION

The geological position of the Blekinge-Bornholm province (BBP) has been under discussion for almost three decades. According to Wiklander (1974) rocks of the BBP should be older than the bordering Småland granites in the north. Based on this hypothesis, Gaál and Gorbatschev (1987) did not include the BBP in the today's Transscandinavian Igneous Belt (TIB). The Småland granites thus represent the southernmost part of the TIB. Since then the BBP has been considered to be a part of the Svecofennian domain. Johansson and Larsen (1989) presented their isotopic age determination for the Tving granitoids from the Blekinge province. They interpreted the Tving granitoids as a part of the South- West Gneiss Complex (SWG). Recent detail mapping and datings of the Tving granitoids and the southernmost Småland granites (Kornfält, 1993, 1996, 2000) have given similar ages as the TIB rocks. Kornfält (2000) suggested therefore the continuation of the TIB into the BBP. However, a recent study (Lindh et al., 2001) of the Blekinge Shear Zone (BSZ), a major tectonic E-W trending lineament separating the Småland and Tving granitoids, revealed pronounced geochemical differences between those two rock types and suggested different sources of the granitoids on the either side of the BSZ. The same authors proposed the name "Småland-Blekinge Deformation Zone (SBDZ)" for the Blekinge Shear Zone.

According to the recent geological mapping at the scale 1:50 000 of the 3F Karlskrona NO sheet (Kornfält, in press), mafic rocks called as 'unspecified greenstones' form minor massifs widespread across the SBDZ.

My work focuses on a petrological and geochemical comparison of all types of mafic rocks (except the rocks of the ca. 1000 Ma old Blekinge- Dalarna dyke swarm) on both sides of the SBDZ. I have collected samples from an extensive area across the SBDZ. These samples are analysed for major, trace elements (including rare earth elements). I have studied them in thin sections in both optical and scanning electron microscopes. Field and microscopic observations were used to reveal the age relationships between the mafic rocks and their enclosing granitoids. Together with geochemical analyses these methods were applied for the classification and construction of the petrogenetic model of the mafic rocks.

Mafic rocks is a useful tool to reveal, whether the BSDZ separates different terranes or is a superimposed tectonic feature. Mafic rocks, which most probably are derived from the mantle, carry important information on the processes in the mantle; thus they can be used as an indicator of the plate tectonic setting for the magmatism. A geological investigation across the SBDZ using this approach has not earlier been performed.

II. GEOLOGICAL SETTING

The present study area is situated in SE Sweden. It covers the eastern part of the county of Blekinge and extends into the south easternmost part of the county of Småland. Geologically it belongs to the Blekinge-Bornholm province, which comprises a part of SE Sweden and the Danish island of Bornholm (Fig. 1). The bedrock of eastern Blekinge is composed of Proterozoic rocks, mainly granitoids.

The northern part of the area consists of massive coarse-grained Småland-type granites that belong to the TIB (Gaál & Gorbatschev, 1987). The TIB granites of the Småland type in Blekinge and southernmost Småland yield U-Pb zircon ages of ca. 1780-1800 Ma (Kornfält 1993, Kornfält & Vaasjoki, 1999). Porphyritic, weakly migmatized gneissic granites occur at a considerable distance to the south of the SBDZ (Fig.2). Kornfält (1993, 1996) refer to these granites as Filipstad-type granites (variety of the Småland granites) with minimum ages around 1720-1750 Ma.

In the south- eastern part of Blekinge, foliated granite, granodiorite and tonalite, collectively called the Tving granitoids occur. The most common variety is a grey to reddish grey, often microcline megacrysts-bearing granitoid (Kornfält, 2000). The Tving granitoids yielded an U-Pb zircon age of ca. 1770 Ma and

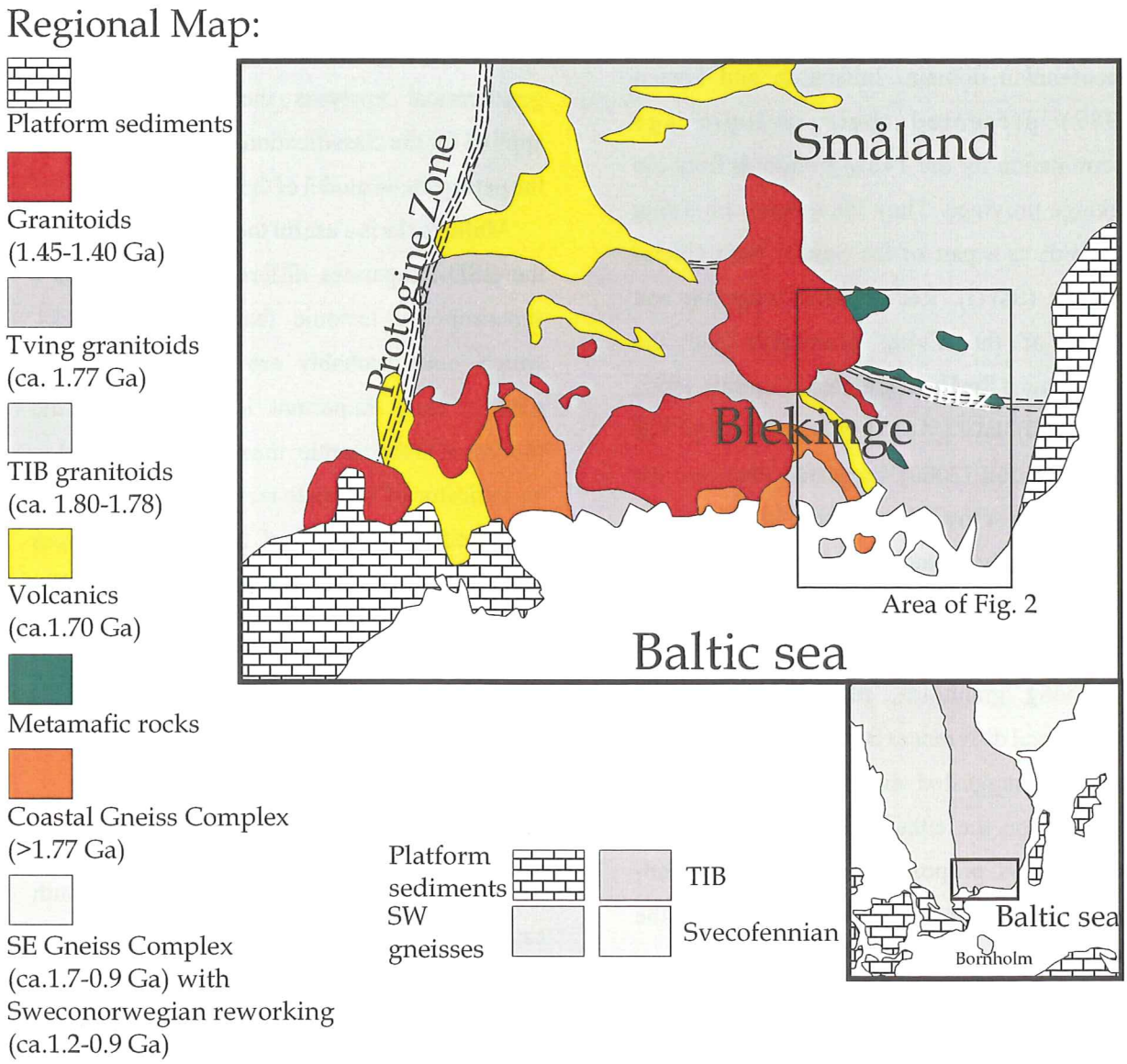

Fig. 1. Major geological units in the Blekinge and southern Småland crustal provinces (modified after Lindh et al. (2001). The inset map shows main geological structures of the Baltic Shield in southern-central Sweden..

were interpreted to belong to the SWG (Johansson & Larsen 1989). A more recent interpretation of the relationship between Småland and Tving granitoids by Kornfält (2000) is in contradiction to the previous ones and suggests that both granite types were formed as a result of the same igneous event within ca. 10 Ma (Kornfält, 2000). Therefore, Tving granitoids are included into the TIB representing its southernmost extent. However, chemical differences suggest different source rocks for the Småland and Tving granitoids (Lindh et al., 2001).

In addition to these major geological units, the coastal gneisses and varieties of the leucocratic granites, locally named Jämjö and Almö granites, should be mentioned, which are minor geological units in the studied area (Fig.2). Varieties of these leucocratic granites yielded ages around 1.75 Ma (Kornfält, 1996). According to field interpretation the coastal gneiss, which is significant geological unit to the west of studied area, is supposed to be the oldest unit in the area. However, a U-Pb multi-grain zircon age determination of Johansson and Larsen (1989) gave a discordant upper intercept age of 1690±39 Ma. They considered the possibility that complex zircons in the coastal gneiss are responsible for this young age. The youngest unit in the region (except the rocks of the ca. 1000 Ma old Blekinge- Dalarna dyke swarm) is the coarse grained, K-feldspar megacrysts-bearing Karlshamn and Eringsboda granitic intrusions, fine- and even-grained Spinkamåla and Vånga granites. The age determinations of these granites yielded ages around 1400-1450 Ma (Kornfält, 1996, Kornfält & Vaasjoki, 1999, Geisler & Schleicher, 2000).

The most important tectonic feature of the area is the SBDZ. The degree of deformation within the SBDZ varies widely from foliated, but still recognisable country rocks to banded mylonites. Lindh et al. (2001) even suggested the occurrence of devitrified pseudotachylite. This approximately EW-trending zone separates the TIB Småland-type granitoids from the Tving ones. 'It is unclear, whether the SBDZ continuous to the west of the Eringsboda massive, and even more questionable, whether it could be considered as a terrane boundary' (Lindh et al., 2001).

Small bodies of amphibolites and metagabbros (the object of this work) are scattered throughout the investigated area. In SGU maps, they are shown as "unspecified greenstones" (Kornfält, 2000). Most of these "greenstones" vary from strongly foliated to undeformed fine- to medium-grained metamafic rocks. Some minor bodies of medium-grained metagabbro and coarse-grained olivine-bearing gabbro are present. Similar mafic rocks occur on both sides of the SBDZ. The mafic rocks are, so far, only poorly studied and their internal relationships are uncertain. The only radiogenic dating on these rocks was performed by Johansson & Larsen (1989) using the whole-rock Rb-Sr method. A reference line for the mafic rocks and for the enclosing rocks gave an age of 1666 Ma, suggesting that the main metamorphism occurred in rather close connection with the rock forming event. (Johansson & Larsen, 1989). However, Kornfält (2000) based on field observations suggests that most of "greenstones" on both sides of the SBDZ are somewhat older than the surrounding granites.

III. Methods and Results

1. Field observations

1.1 Field description

During the field work in eastern Blekinge and southern Småland, I have examined small but widespread massifs of mafic rocks on both sides of the SBDZ. Kornfält (2000) described the different kinds of mafic rocks as "greenstones" (SGU 3F Karlskrona NO map-sheet). Several small, scattered massifs of mafic rocks occur across the SBDZ (Fig. 2). They are, however, somewhat concentrated into four main areas: to the north of the SBDZ: (1) an approximately E-W trending 5 to 10 km wide zone parallel to the SBDZ, (2) an E-W trending zone north of Holmsjö; to the south of the SBDZ: (3) a number of massifs to the southwest and to the southeast of Rödeby and (4) a belt of several massifs to some extent following a NW direction from Sturkö Island through Karlskrona to Nättraby (Fig.2).

Exposures of the mafic massifs in the investigated area are poor; therefore, the true size of the massifs is impossible to determine in most cases. Some of the massifs can only be observed in a single outcrop and examinations of their contacts with the host granitoids are limited.

The orientation of the foliation in the mafic rocks and the granitoids was recorded in the field. Structural data were plotted in StereoNet light version 3.03 (Fig. 3). The distribution of the plotted poles shows that the foliation of the metamafic rocks and the granitoids coincides. This suggests that the deformation that caused the foliation in both rock types was regional and affected both rocks types after their crystallisation.

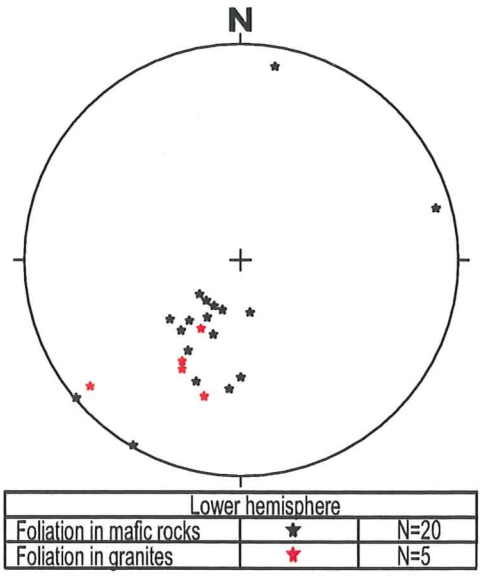

Fig. 3. The orientation of the foliation in the mafic rocks and granitoids in the studied area plotted on lower hemisphere of an equal area projection. (Software: StereoNet light version 3.03)

Legend to Fig.2 on next page

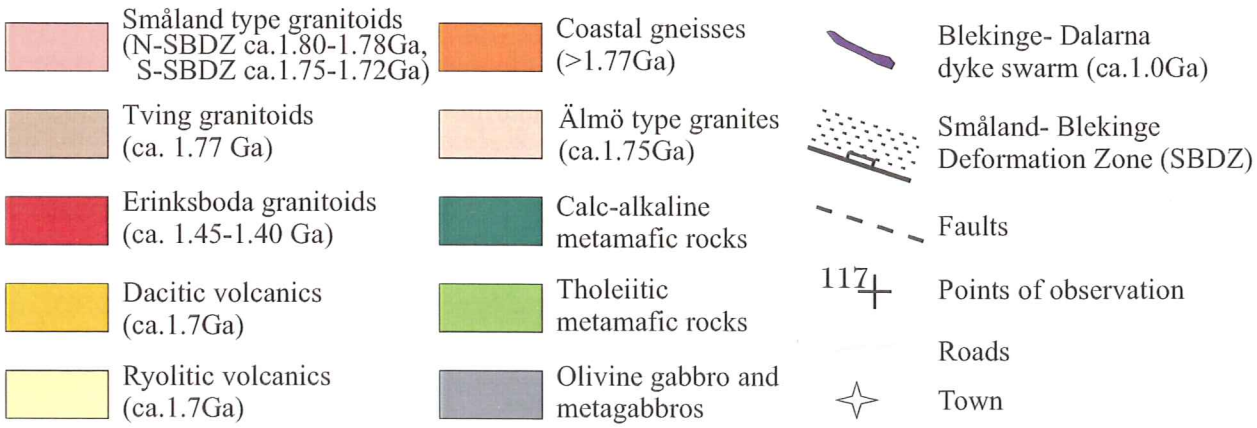

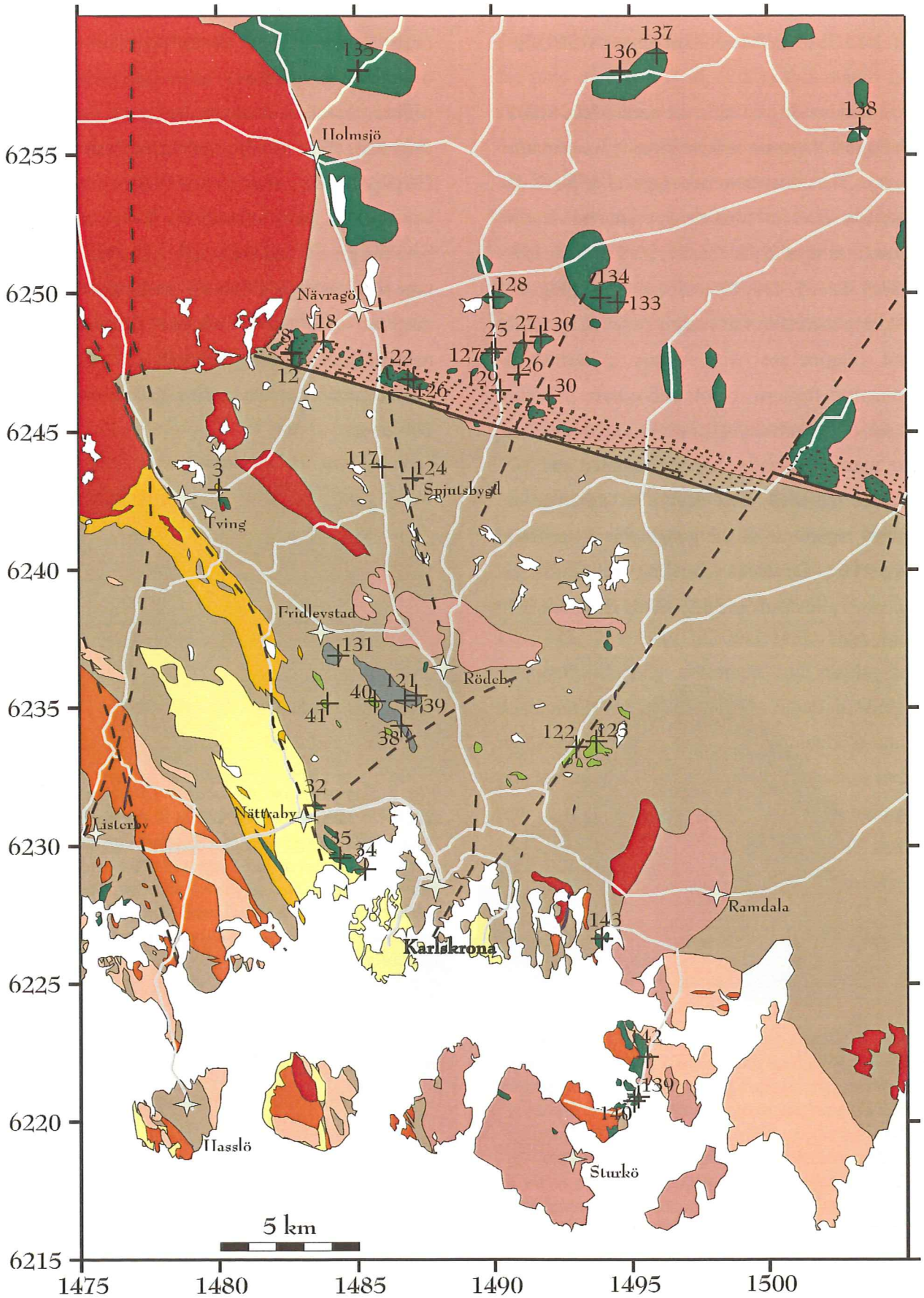

Fig. 2. Geological map of the eastern Blekinge province (modified after Kornfält and Bergström (1990), Kornfält (in press) and Lindh et al. (2001). The lithological boundary between the Småland granites and Tving granitoids from Kornfält (in press). The Småland-Blekinge Deformation Zone from Lindh et al. (2001). Coordinates: the Swedish grid with the RT90 coordinates system.

1.1.1 The Northern Subprovince (N-SBDZ)

Field investigations to the north of the SBDZ show that there are at least three types of mafic rocks. The most common type is a black or greyish, fine- to medium-grained, metamafic rock (localities 22, 25, 26, 27, 30, 126, 127, 128, 129, 130, 133, 134, 135, 136, 137, 138; Fig. 2). Major minerals in this rock type are amphibole and plagioclase with minor amounts of potassium feldspar, biotite and quartz. In some cases, most probably, phenocrysts of plagioclase are present. Usually they are rounded and 1-2 mm in diameter. The degree of deformation varies regardless of the geographical position. Important localities showing relationships between granitoids and metamafic rocks are 137 and 138.

Fig. 4. Sample from the locality 137 from the N-SBDZ. Mingling and localised mixing between granites and metamafic rocks. Irregular shape and diffuse, 'dissolved' contacts are typical for the fragments of the metamafic rock. They are incorporated in a fine grained matrix of intermediate composition, which looks to be a hybrid rock between granite and metamafic rock. Box of snus (7cm in diameter) for scale.

At locality 137 mingling and localized mixing between granitoids and metamafic rocks occur. The size of the metamafic fragments ranges from a few centimetres to a few decimetres in diameter. The irregular shape and diffuse, 'dissolved' contacts are typical for these fragments (Fig. 4). They are incorporated in a fine-grained matrix of intermediate composition, which looks as a hybrid rock between granite and metamafic rock, and which may represent a local mixing product of the two magmas. The direct contact between the mingled part and the granitoids is not exposed but the granite crops out at the distance of about 10 metres.

Fig. 5. Sample from the locality 138 from the N-SBDZ. A direct contact between the metamafic rock and the granitoid. At the contact, the granitoid has an about 2 cm wide rim where it is recrystallised into a more fine grained and darker (probably hybrid) rock. Fragments of the same hybrid rock are incorporated into the metamafic rock as well. Box of snus (7cm in diameter) for scale.

At locality 138 the mingling and localized mixing situation are similar to those described above. Additionally, a few large K-feldspar crystals with diameter of 2cm seem to be incorporated into the surrounding intermediate matrix. They most probably derive from the adjacent granite, which contains large K-feldspar crystals. A direct contact between the metamafic rock and the granite is also present. At the contact, the granite is recrystallised into a

more fine grained and darker (probably hybrid) rock in an approximately 2 cm wide zone (Fig. 5). Fragments of the same hybrid rock are included into the metamafic rock as well. Therefore these relationships show that the granitoids and metamafic rocks (at least at these two localities) originate from the same magmatic event.

To the south of Nävragöl (localities 8, 12 and 18), metamafic rocks define a massif that is close to the triple junction between the Småland, Tving and Eringsboda granitoids. One type of these rocks (locality 12) is porphyritic. The megacrysts are made up of amphibole, approximaly 5 mm in diameter, set in fine-grained matrix, which constitutes about 30% of the rock. The second type is a medium-grained metamafic rock (localities 8 and 18), which is more coarse-grained than the majority of the N-SBDZ metamafic rocks. The entire massif shows a complex structure. Penetrative net-like agmatitic veining occurs at localities 8 and 12 (Fig. 6). At the periphery of this massif only minor enclaves of fine-grained metamafic rocks occur within foliated granitoids. Most of these metamafic rocks are strongly foliated. The orientation of the foliation varies, but an E-W direction seems to be dominating. According to the map of Lindh et al. (2001) this massif is situated within the SBDZ. The intense deformation is caused by movements along the SBDZ. The Eringsboda granite intrusion, at the present erosion level, is at a distance of 1 to 2 km to the west of the massif. Such a large intrusion must have given a contact metamorphism input on the metamafic rocks in the surroundings of the intrusion.

1.1.2 The Southern Subprovince (S-SBDZ)

Field observations in the S-SBDZ show wide petrological varieties of mafic rocks. Fine-grained black to dark- grey metamafic rocks are most common (localities 32, 34, 35, 40, 41, 117, 122, 123, 124, 140, 142 and 143). They are frequently ductilly deformed and display a dominant NW-SE steep dipping foliation. These rocks are mainly composed of amphibole and plagioclase with smaller amount of biotite and rare quartz. Contacts with the surrounding granitoids were observed at localities 117 and 124. The granitoids and metamafic rocks in these

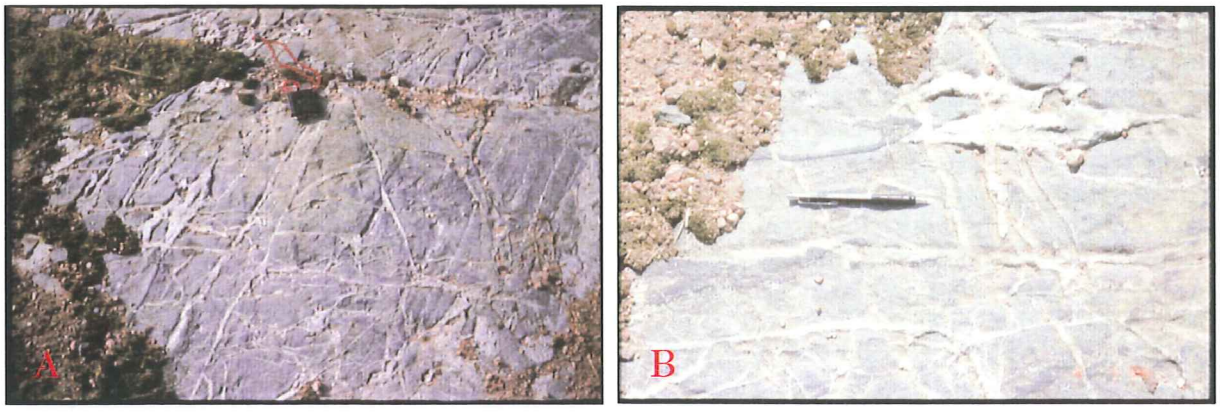

Fig. 6 A and B. Locality 8 in the N-SBDZ. Penetrative net-like agmatitic veining. In figure 6B, black veins of unidentified composition cutting the metamafic rock are deformed and crosscut by the agmatitic veins. Pencil (14 cm long) and compass for scale

localities show mingling and localized mixing relationships as described above for the N-SBDZ rocks (localities 136 and 137).

Fig. 7. Locality 117 in the S-SBDZ. The brecciated metamafic rock. Fragments of the metamafic rock vary in size from small, centimetre- sized fragments to almost half a meter fragments. The shape of the fragments is angular and sharp. The matrix is a homogeneous, greyish, fine-grained rock, intermediate in composition. Sometimes the matrix material is filing millimetre- scale fractures in the metamafic rock fragments. The contact with the granites is along a tectonic fracture. Hammer for scale.

At locality 124, the contact between the metamafic rocks and the granitoids has been examined in blocks remaining after the road construction. The metamafic rocks are homogeneous, fine-grained and black without any signs of deformation. At the contact with the granite, the metamafic rocks are brecciated. Brecciation gradually increases towards the contact. Fragments of the metamafic rocks usually are subrounded with 'dissolved' contacts. The breccia matrix is made up of an intermediate light-grey hybrid rock in some cases with needles of amphibole, which are of few centimetres long. The contact between the matrix of the breccia and the adjacent granite is gradual. The gradual contact zone can be traced at a distance of 2 centimetres into the host rock.

A few kilometres to the west, at the very spectacular locality 117, similar relationships are seen at a larger scale. Two dyke-shaped bodies of the metamafic rocks of approximately five meter width crop out along the road and can be traced for a few hundred meters in the E-W direction. Surrounding rocks are typical Tving granitoids. These dykes are composed of the homogeneous fine-grained metamafic rocks, which is typical for the S-SBDZ. In the northern part of the road cutting, the metamafic rock is brecciated to various degrees. The fragment/matrix ratio gradually decreases towards the contact with the granite. Fragments of the metamafic rock vary in size from small, centimetre-sized fragments to almost half-a-meter fragments (Fig. 7). The shape of the fragments is angular and sharp; clearly different from those at locality 124. The matrix is a homogeneous, greyish, fine-grained rock, intermediate in composition. Sometimes the matrix material fills millimetre-scale fractures in the metamafic fragments. The contact between the matrix rock and the granite forms a few centimetres wide transition zone (Fig. 8).

Fig. 8. Locality 117 in the S-SBDZ. The contact between the brecciated metamafic rock and granitoid. The contact between the matrix of the breccia and the adjacent granitoid is gradual. The extent of the gradual contact zone can be traced at a distance of 2 centimetres into the granitoid. Hammer for scale

Olivine gabbro

A massif of mafic rocks that is situated SW of Rödeby deserves special attention. Compared to the other mafic rock bodies, this is a large massif and the only place in the study area, from which medium to coarse-grained, black olivine-bearing gabbro (locality 39 on Fig.2) has been described (Kornfält, 2000). Deformed and metamorphosed metagabbro occurs at the periphery of this massif (localities 38 and 121). At the locality 121 the metagabbro is porphyritic and composed mainly of large crystals of amphibole. A similar porphyritic metagabbro forms a separate massif a few kilometres to the NW of the Rödeby massif (locality 131).

A porphyritic metamafic rock was observed along the road to Sturkö Island (locality 139). This porphyritic metamafic rock gradually changes to a fine-grained metamafic rock similar to the other S-SBDZ fine-grained metamafic rocks. The amphibole crystals sometimes reach five centimetres in diameter. The fine-grained matrix of the porphyritic metamafic rock is composed mainly of amphibole and plagioclase together with rather large (up to 0.5 cm) K-feldspar crystals. The amphibole and the K-feldspar crystals are irregularly distributed. It is probable that K-feldspar could be xenocrystic and deriving from the surrounding granitoids.

A particular fine-grained variety of the metamafic rock is observed near Tving (locality 3). It is a dark grey, ductilly deformed rock with a distinct foliation. It is mainly composed of plagioclase, biotite and accessory quartz and amphibole. The rock has a microlayering of comparatively lighter and darker layers.

1.2 Magnetic susceptibility measurements

Magnetic susceptibility (MS) measurements of mafic rocks and surrounding granitoids were performed to test, whether the high magnetic anomalies on the aeromagnetic map (sheet 3F Karlskrona; scale 1: 100 000; SGU, 1999) correspond to the location and shape of the mafic rock massifs (Fig. 9).

Most of the granitoids on both sides of the SBDZ show similar values of MS in the range 1000-3000 nTl; the most common value being around 2000 nTl. However, the MS values for the metamafic rocks scatter. In respect to MS three major groups of the metamafic rocks are distinguished with: (1) less than 100 nTl, (2) 100-1000 nTl and (3) more than 1000 nTl (Table 1). These groups are characteristic for different massifs, but may also be found within a single massif. A direct correlation between the outcrop MS and the aeromagnetic anomalies has not been found. In some cases, rocks with high MS are situated within areas of a magnetic low and *vice versa*. The large MS intramassif variation

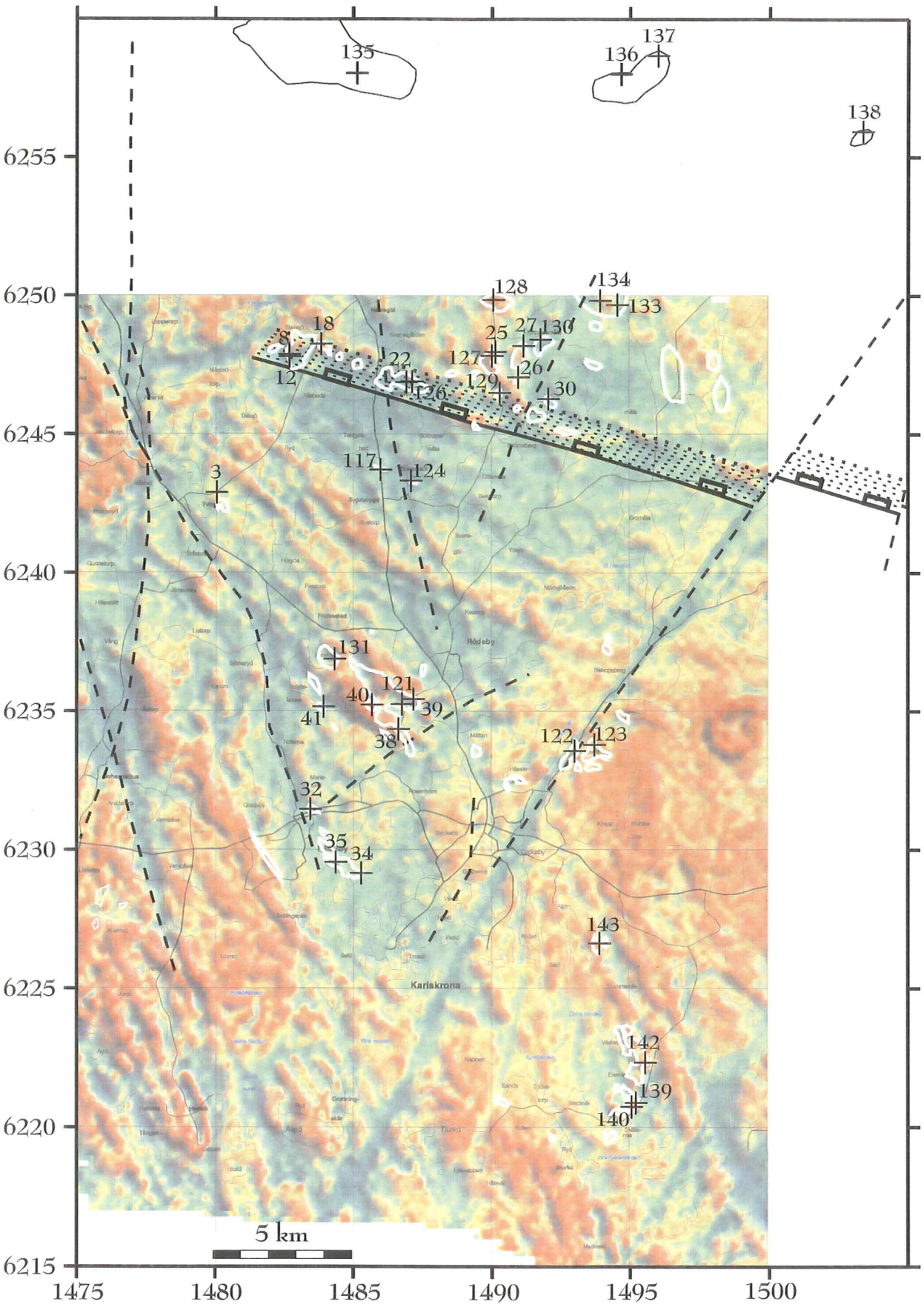

Fig. 9. Airbone magnetic anomaly map (SGU, 1999). The shape of the massifs (white lines) of metamafic rocks from Fig. 2. Magnetic highs are in red- and lows in blue colours.

prevents me from drawing the massif boundaries based on aeromagnetic anomalies.

The magnetic susceptibility (MS) measurements failed to correlate the aeromagnetic data to the location and geological boundaries of the mafic rocks. The MS depends on the quantity of magnetic and paramagnetic minerals in the rocks. Therefore, uralitization of pyroxenes and olivine leads to a change of the MS. Appearance of secondary amphibole after pyroxene and olivine is most obvious in the samples of the olivine gabbro and metagabbro. Replacement of pyroxene by amphibole was observed in a few samples of fine-grained metamafic rocks as well. Deformation associated with mineral changes (for example appearance of titanite) will also influence the MS. Therefore the large variation of the MS within one massif are most probably due to the metamorphic and/or deformation controled mineralogical changes.

2. Petrography and Mineralogy

The studied metamafic rocks to the north and to the south of the SBDZ, described petrographically as separate groups, have similar mineral compositions. The dominant phases are plagioclase and amphibole with various amounts of biotite and ore minerals. The studied metamafic rocks are characterized by minor variations in the grain size. Two groups of the metamafic rocks can be distinguished based on grain size. The first one is a fine- to medium-grained (0.5-2 mm grain size) rock, which is uniform in mineral composition and texture. The second group comprises porphyritic metamafic rocks, in which up to 5 cm large crystals of amphibole are present. The porphyritic metamafic rocks are similar in appearance, and occur in close spatial relationships with the fine-grained metamafic rocks. There is a unique olivine bearing gabbro massif to the west of Rödeby, which represents a separate group in this description. The fresh olivine gabbro together with the coarse-grained metagabbro makes up a large massif to the west of Rödeby in the S-SBDZ.

The brecciated variety of common type fine-grained metamafic rock, that has been found in the S-SBDZ (localities 117, 124) and the N-SBDZ (localities 137, 138), has a similar appearance at all localities. The detailed petrographic description of the brecciated rocks has been performed for locality 117.

Point counting results from all the thin section are given in Table 2.

2.1 The Northern Subprovince

Fine- grained metamafic rocks

The fine-grained metamafic rocks mostly are equigranular and in some cases (localities 135 and 138) they show ophitic textures. Deformation and metamorphism are weak. A clear foliation can be seen at some localities (localities 22 and 126).

Major minerals are plagioclase, amphibole, biotite and ore minerals. In most of the samples, several types of plagioclase exist. Comparatively large (1-2 mm in diameter) grains of euhedral plagioclase with clear zonation are common in some samples (localities 26, 135, 138, 127 and 128). Fine-grained subhedral plagioclase with either clear

or weak twinning is present in most of the samples. Potassium feldspar is absent in most of the rocks except for one specimen (locality 22), where it is present in significant amounts; probably as a magmatic phase. Amphibole is typically fine grained and anhedral. In the foliated rocks (localities 22 and 126), amphibole exhibits a preferred orientation. In the metadolerite (locality 135), amphibole replaces intensely uralitizated clinopyroxene. Biotite occurs as subhedral or anhedral grains. Most of the rocks contain small amounts of quartz. Accessory magnetite is mostly anhedral. In some of the metamafic rocks (locality 135), magnetite formed as a reaction product between amphibole and biotite. Euhedral magnetite was observed in few specimens (localities 26, 127, 128 and 130) as well. Accessory apatite is present in all the rocks and occurs as fine needles, included in all major minerals. Titanite is rare and represented by euhedral dark brown grains in least deformed rocks (localities 135,136 and 138), most probably, as primary mineral. Minor, lighter secondary titanite is most common in the foliated metamafic rocks (locality 22). Epidote in most samples replacing plagioclase. Zircon is present as single, non-transparent grains in few samples (localities 22, 26 and 130).

Porphyritic metamafic rocks

The porphyritic metamafic rock (locality 12) is composed of large (up to 5 mm) megacrysts of amphibole embedded in a fine-grained matrix (Fig. 10). The megacrysts are anhedral, rounded grains that usually do not impinge on each other. Microprobe analyses show that the amphibole megacrysts have a magnesio-hornblende composition (Table 3). The amphibole is green to dark green and inhomogeneous in appearance. Inclusions of anhedral titanite, epidote and plagioclase are common. The composition of the plagioclase inclusions varies, most common phases are labradorite and oligoclase (Table 4). Some grains of plagioclase contain inclusions of

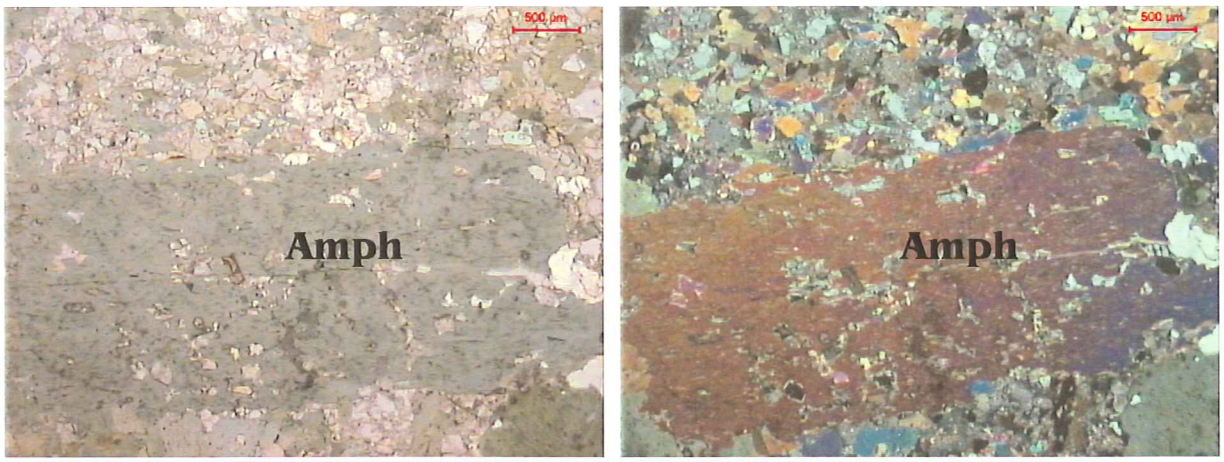

Fig. 10. Microphotographs of the N-SBDZ porphyritic metamafic rock (locality 12) composed of large (up to 5 mm) megacrysts of amphibole embedded in a fine-grained matrix. The megacrysts are anhedral, subrounded grains and usually do not have any contact with each other. The amphibole composition is magnesio-hornblende. The matrix is composed of anhedral, fine-grained magnesio- or actinolitic hornblende, clinopyroxene, plagioclase, quartz and rare potassium feldspar and biotite. Scale bar is 500 µm.

potassium feldspar and biotite.

The matrix of the porphyritic metamafic rocks is made up of anhedral, fine-grained magnesio- or actinolitic hornblende, clinopyroxene, plagioclase, quartz and rare K-feldspar and biotite. The clinopyroxene is of the diopside-hedenbergite series with the composition of Cpx $_{(En\ 35\text{-}37;\ Fe\ 11\text{-}13;\ Wo\ 51)}$ (Table 4). The matrix plagioclase is an andesine (Table 4) and different in composition to plagioclase inclusions in amphibole megacrysts.

2.2 The Southern Subprovince

Fine-grained metamafic rocks

The S-SBDZ fine-grained metamafic rocks are composed of amphibole, plagioclase and biotite as dominant phases. In addition, small amounts of quartz are present in some specimens (localities 32, 34, 35 and 41). All rocks have an equigranular texture. Deformation is generally weak and foliation is visible only in few samples (localities 32 and 123). Plagioclase forms mostly anhedral, rounded grains with or without twinning. Larger, zoned plagioclase grains are rare and present only in few samples (localities 35 and 124). Sericitization of plagioclase is common.

Amphibole grains are anhedral and rounded. Inclusions of magnetite and titanite in amphibole are common. Few large amphiboles (e.g. locality 40) have a uralitizated clinopyroxene cores (compositions in Table 7).

Biotite is mostly subhedral, elongated grains with strong pleochroism. Some biotite is either replacing amphibole or forming individual grains both having weak pleochroism. In the foliated rocks, biotite shows a preferred orientation parallel to the foliation.

Magnetite is very rare and in some cases forms anhedral but rather large grains (locality 122). The tiny grains of magnetite grown within the amphibole. Fine needles of apatite are present in all the major minerals. Anhedral grains of titanite are secondary and partly replacing the amphibole. Zircon is rare.

Porphyritic metamafic rocks

Porphyritic metamafic rock was observed at locality 139 in the S-SBDZ. It is close spatial relationship to the fine-grained metamafic rocks. Megacrysts of amphibole are 1 to 5 cm in diameter. The megacrysts are anhedral with diffuse contacts to the matrix. They do not impinge on each other. Amphibole megacrysts are rich in relicts of clinopyroxene and orthopyroxene. Inclusions of small anhedral plagioclase are common. Rare inclusions of biotite are mostly at the periphery of the megacrysts.

The matrix is composed of anhedral amphibole and plagioclase. Amphibole makes up ca. 70% of the matrix and frequently has uralitizated pyroxene inclusions. Comparatively large, grains of K-feldspar were observed within the matrix. Rare, small subhedral grains of magnetite occur both in the matrix and as inclusions in the megacrysts.

Olivine gabbro

The olivine gabbro at locality 39 is a black coarse-grained totally undeformed rock. The gabbro is composed of cumulative olivine and

plagioclase, and interstitial orthopyroxene and clinopyroxene. Amphibole, spinel, phlogopite and magnetite were formed as later reaction products between the cumulative and interstitial minerals. Plagioclase forms comparatively large, subhedral crystals with clear and distinct twins. It is extremely rich in the anorthite component. The average composition of the plagioclase is bytownite Pl $_{(Ab\ 15\text{-}17;\ An\ 82\text{-}85)}$. In some cases it is almost pure anorthite Pl $_{(Ab\ 3\text{-}9;An\ 90\text{-}97)}$. The plagioclase shows no zonation and composition varies within one crystal without sequence. Small inclusions of secondary amphibole are common (Table 5).

Olivine forms small, subrounded grains, which are anhedral and strongly fractured. The composition of olivine is almost uniform throughout the gabbro (Table 5). The Mg# (magnesium number) is about 0.65. The secondary, very fine-grained magnetite are found within cracks in the olivine (Fig. 11). A thin rim of granular, elongated orthopyroxene that is radially oriented to the olivine grains surrounds most of the olivine (Fig. 12). Orthopyroxene is most probably interstitial and forms rims around the olivine independently of what mineral contacts the olivine. Olivine appears to have acted as a nucleus for the orthopyroxene crystallization from the melt. Orthopyroxene is hypersthene with the composition Opx $_{(En70\text{-}71,\ Fe27\text{-}28,\ Wo0.5)}$ (Table 5). At the olivine-hypersthene contact, the fine-grained magnetite occurs.

Olivine shows spectacular reaction rims or kelyphytic coronas at the contact to plagioclase. Kelyphytic coronas formed by a reaction between olivine and plagioclase and are composed of symplectitic intergrowth of amphibole and spinel (Fig. 12). Amphibole is of diverse compositions from pargasite to hornblende or tschermakite (Table 6) and forms more than 70% of the symplectite. Rare inclusions of phlogopite (Table 5) are present. Separately, kelyphytic amphibole developed in between the symplectite and the orthopyroxene layer.

Spinel composition is close to pure ferroan spinels (Table 5). In more altered gabbro the kelyphytic corona are more evolved and, in some cases, totally substitute plagioclase. The

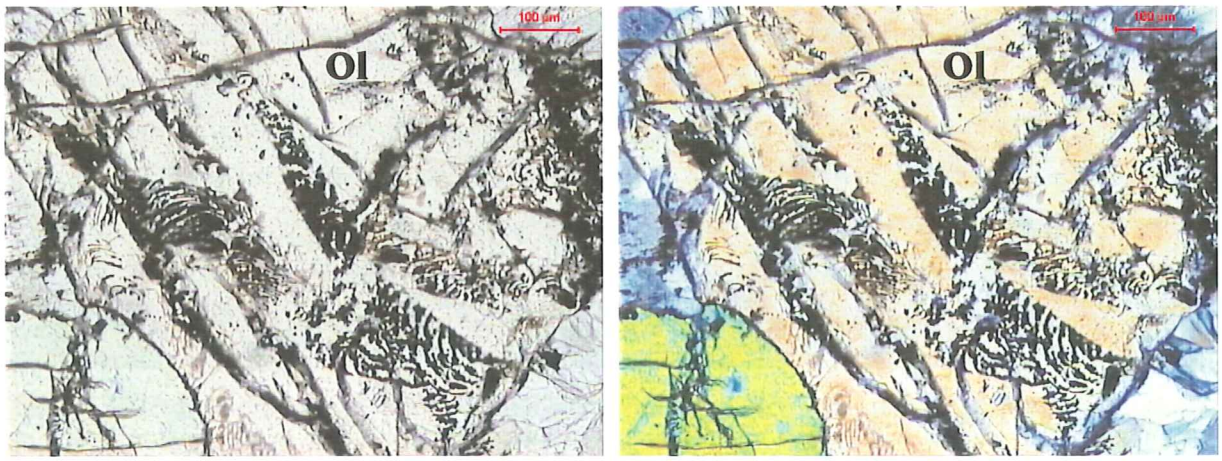

Fig. 11. Microphotographs of the olivine gabbro of the Rödeby massif in S-SBDZ, locality 39. Exsolution of the most fine-grained magnetite in olivine. Scale bar 100 μm.

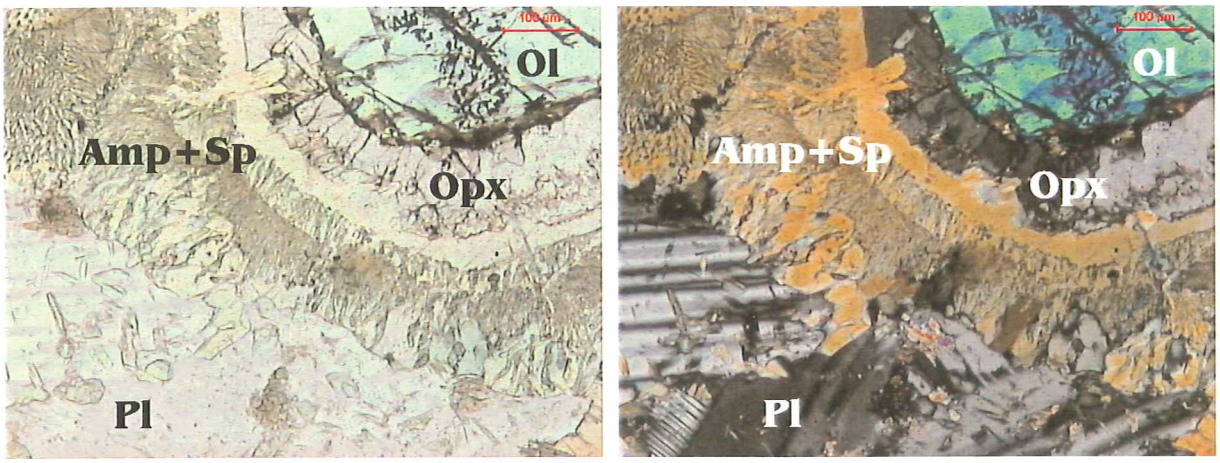

Fig. 12. Microphotographs of the olivine gabbro of the Rödeby massif in S-SBDZ, locality 39. A thin rim of granular elongated orthopyroxene that is radially oriented to the olivine grains surrounds the olivine. At the contact between olivine and orthopyroxene the exsolution of magnetite occurred. Reaction kelyphytic coronas between olivine and plagioclase are composed of symplectite intergrowth of amphibole and spinel. Amphibole is of diverse compositions and forms more than 70% of the symplectite. Separately, kelyphytic amphibole developed in between the symplectite and the orthopyroxene layer. Scale bar is 100 μm.

further development of the symplectite caused the symplectite intergrowth of amphibole and spinel to separate into two independent phases.

Clinopyroxene is present as an interstitial phase and forms rather large grains with a composition of Cpx $_{(En44-45,\ Fe7-8,\ Wo46-47)}$ (Table 5). Replacement of clinopyroxene by amphibole of a similar composition to that in the kelyphytic symplectites is common. Clinopyroxene contains earlier crystallized small grains of plagioclase and olivine as inclusions. In this case a thin rim of amphibole usually surrounds the plagioclase. Similar rims exist around olivine and are composed of amphibole together with very fine-grained magnetite (Fig. 13). The clinopyroxene is generally altered and partly substituted by amphibole and phlogopite.

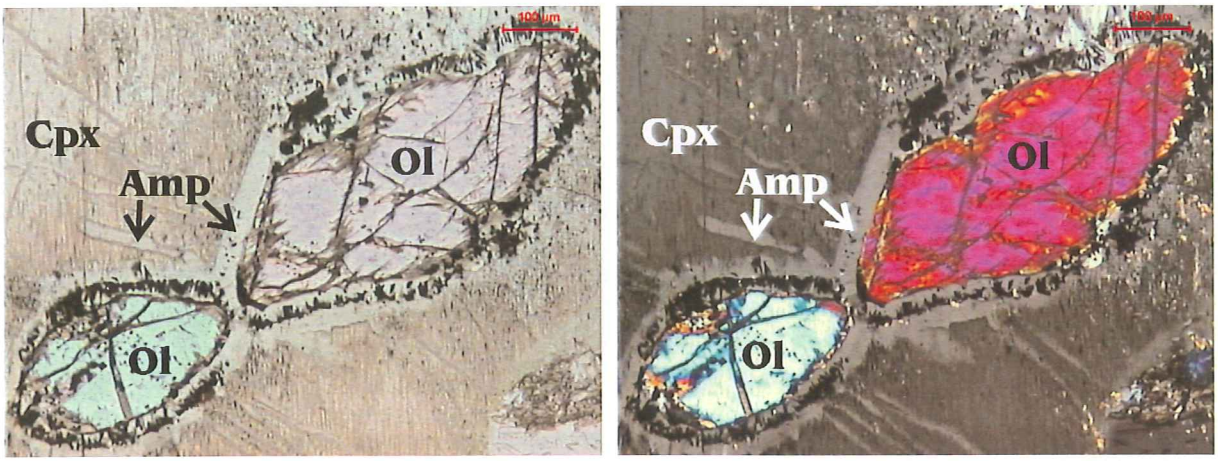

Fig. 13. Microphotographs of the olivine gabbro of the Rödeby massif in S-SBDZ, locality 39. Clinopyroxene as an interstitial phase containing earlier crystallized olivine. A thin rim of amphibole is usually surrounding the olivine and is composed of amphibole together with very fine-grained magnetite. The clinopyroxene is generally altered and substituted by amphibole in some parts. Scale bar is 100 μm.

Coarse-grained metagabbro

Coarse-grained metagabbro was observed at a few localities (localities 38, 121 and 131) within and near the Rödeby massif. The rock has an ophitic or porphyritic texture. The degree of deformation varies from massive to foliated. The major minerals are amphibole and plagioclase. Amphibole makes up ca. 50-70% of the rock. It differs in size and forms subhedral or anhedral grains. Some large amphibole grains have relicts of clinopyroxene in the cores. Clinopyroxenes are strongly uralitizated. Plagioclase is sub- or euhedral with strong sericitization. Zonation is rare. Accessory minerals are biotite, apatite, magnetite and titanite.

Brecciated metamafic rock

Samples have been taken from different parts of the breccia: (i) fine grained black fragments of metamafic rock (sample 117-4), and (ii) fine-grained grey matrix from the fragment-rich breccia (sample 117-3).

The fine-grained black metamafic rock is similar to other metamafic rocks from the S-SBDZ. It is composed of amphibole and plagioclase as major phases. The amphibole forms subhedral grains with rare inclusions of biotite. At least two different kinds of amphiboles can be observed in one single thin section (Table 8). Plagioclase is anhedral and strongly sericitizated with a weakly developed twinning. Plagioclases of two different compositions are present. One type is oligoclase-andesine and the other one is labradorite to bytownite (Table 9). Biotite is usually subhedral and elongated, but has no clear preferred orientation (composition in Table 9). Accessory titanite is anhedral and forms comparatively large grains. Magnetite is rare. Few, big anhedral grains of K-feldspar are observed. K-feldspar displays 'dissolved' contacts and possess an irregular shape (Fig. 14). The K-feldspar grains are probably xenocrysts assimilated from the surrounding granitoids.

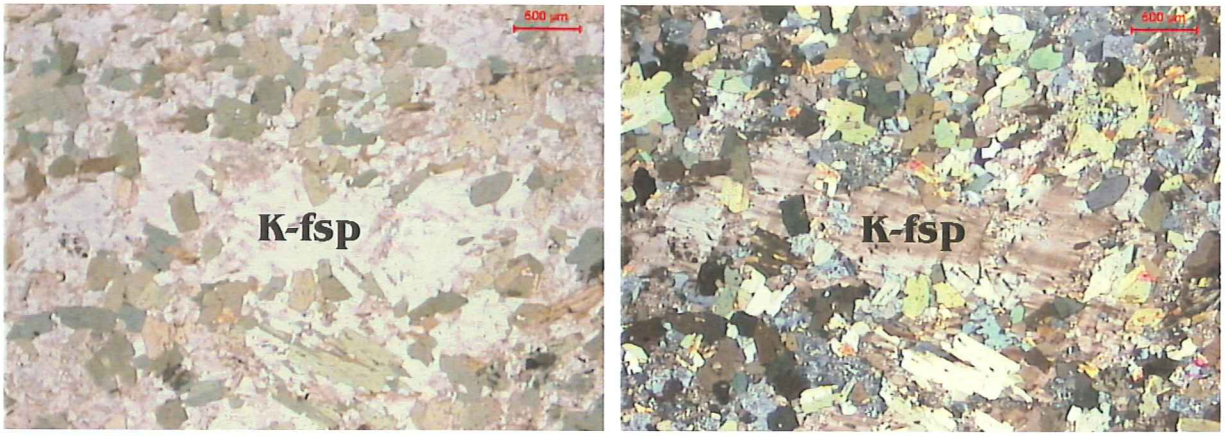

Fig. 14. Microphotograph of the fragments of the brecciated fine-grained metamafic from the S-SBDZ, locality 117. It is composed of amphibole and plagioclase as main phases. The amphibole forms subhedral grains with rare inclusions of biotite. Plagioclase is anhedral and strongly seritizated with a weakly developed twinning. A large anhedral grain of potassium feldspar in the centre of the picture displays 'dissolved' contacts and possesses an irregular shape. Scale bar is 500 μm.

The fine-grained, grey, intermediate matrix is composed of plagioclase, quartz, K-feldspar and biotite as major phases. Plagioclase of two different compositions, andesine and albite is present (Table 10). In addition, there are rare grains of amphibole and magnetite. Amphibole has a uniform composition, which is similar to those of the amphibole from the metamafic fragments (Table 8). Secondary titanite is mostly anhedral but a few euhedral grains are present. Secondary fine-grained epidote replaces plagioclase.

To summarize the petrographic description: four different groups of metamafic rocks can be distinguished with the distinct mineralogy and textures:

(1) Fine-grained metamafic rocks. Petrographically similar metamafic rocks exist on both sides of the SBDZ.

(2) The porphyritic metamafic rocks, which appears on both sides of the SBDZ in the close spatial relationship to the fine-grained metamafic rocks.

(3) The coarse-grained olivine gabbro and (4) the coarse-grained metagabbro, which together comprise a Rödeby massive in the S-SBDZ.

3. P-T estimates of the brecciated metamafic rocks

Microprobe analyses of amphibole have been used for pressure estimation. The set of total aluminum in amphibole geobarometers of Hammarstrom & Zen (1986), Hollister et al. (1987), Johnson & Rutherford (1989) and Schmidt (1992) was applied on the mineral analyses. The different methods suggest a variation in pressures of about 2 kbar for the same sample.

The geobarometer based on total Al in amphibole was applied on the brecciated rocks from locality 117. The amphiboles from the metamafic rock fragments and the intermediate matrix give similar results even if amphiboles compositions vary. The pressure estimated for the metamafic rocks is in the range of 4.7-6.9 kbar and for the intermediate matrix in the range of 5-7.3 kbar. However, one amphibole from the metamafic rock gives unreliable high pressure of 12 kbar.

The amphibole-plagioclase thermometer calibrated by Holland and Blundy (1994) was applied for the same rocks as well. The temperature estimation for the fragments of the metamafic rock and the intermediate matrix gave similar temperatures of 600 to 870 °C for both rocks.

4. Geochemistry

4.1 Analytical technique

Analyses of major and some trace elements have been performed at the chemical laboratory of the Ernst Moritz Arndt University, Greifswald (Germany) with the XRF method by Z. Solyom. Trace elements including REE have been analysed by ICP/MS at the ACME laboratory (Canada). Samples for trace elements and REE were dissolved by $LiBO_2$ fusion. The Cu, Pb, Zn, Ni fractions were leached with a HCl-HNO_3-H_2O equal parts mixture at 95°C for one hour and analysed by ICP-ES. The geochemical analyses are presented in Table 11.

4.2 Major elements

4.2.1 Rock classification

Major elements have been used as a basis for the classification of the studied rocks. The total alkalis or K_2O and silica contents are most suitable for the classification of mafic rocks (Rollinson, 1993). There are few diagrams for the subdivision of volcanic rocks in regard to their alkalinity (Le Maitre et al., 1989, MacDonald & Katsura 1964, Rickwood, 1989).

The total alkali versus silica (TAS) diagram (Fig. 15) demonstrates that most of the N-SBDZ metamafic rocks are of basaltic andesitic- to andesitic compositions. The composition variation is small. However, two samples (localities 8 and 18) are clearly different from the rest of the rocks and fall into the field of subalkaline basalts (symbols are not visible on the diagram because they overlapping with the S-SBDZ metamafic rocks).

The majority of the S-SBDZ metamafic rocks have mainly subalkaline basaltic compositions. One sample from locality 3 is dissimilar to the other rocks and plots in the trachyandesite field. Four S-SBDZ metamafic rocks (localities 40, 41, 122 and 123) are different from the rest and falls into alkaline basalts field.

The porphyritic metamafic rocks from both sides of the SBDZ (localities 12 and 139) and the metagabbro (localities 38, 121 and 131) from the Rödeby massif are quite uniform in composition and fall into the subalkaline basalt field. The only analysis of the gabbro (locality 39) plots on the lower boundary of the subalkaline basalt field.

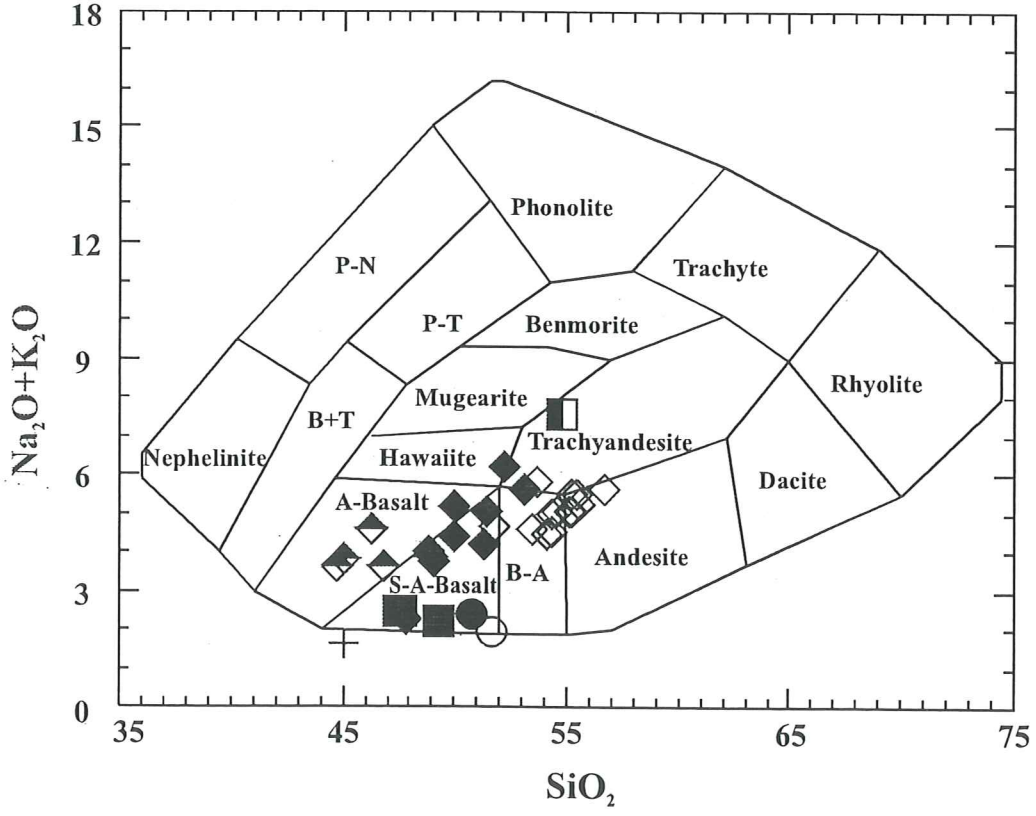

Fig. 15. TAS (total alkalis versus SiO_2) classification diagram for volcanic rocks (Cox et al., 1979). Field abbreviations: B-A basalt andesite, A-Basalt alkaline basalt, S-A Basalt subalkaline basalt. Symbols are on the next page.

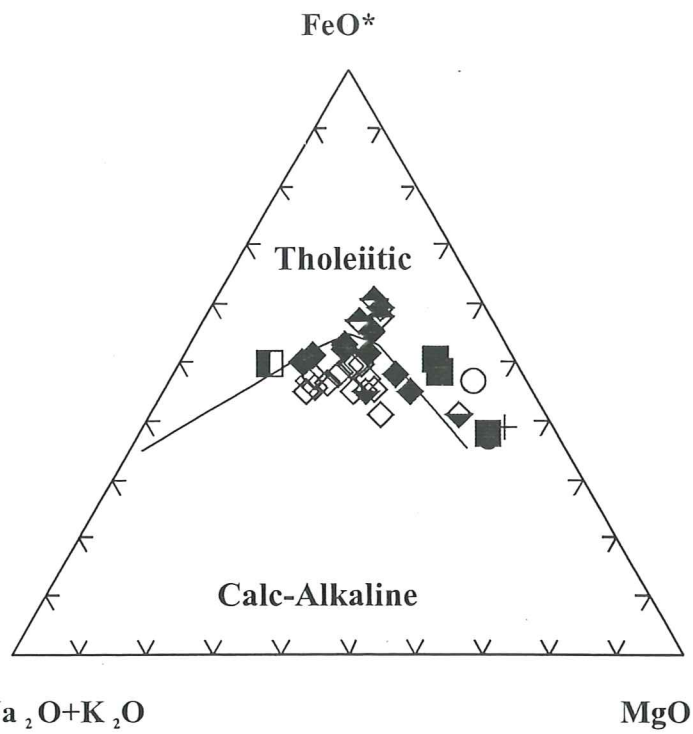

Important:these symbols are valid for all the diagrams.

The N-SBDZ

- ◇ The fine- grained metamafic rocks (calc- alkaline)
- ◆ The fine- to medium-grained metamafic rocks (samples 8 and 18)
- ○ The pophyritic metamafic rock

The S-SBDZ

- ◆ The fine- grained metamafic rocks (calc- alkaline)
- ◆ The fine- grained metamafic rocks (tholeiitic)
- ● The pophyritic metamafic rock
- ■ The metagabbros
- \+ The olivine gabbro
- ◧ The trachyandesitic volcanics

Fig. 16. AFM (alkalis-FeO-MgO) discrimination diagram. The line separating tholeiitic and calc-alkaline series is from Irvine & Baragar (1971).*

All data are plotted in the AFM diagram (Fig. 16; Irvine and Baragar, 1971). The N-SBDZ metamafic rocks plots almost entirely in the calc- alkaline field. Sample 18 is the only one of N-SBDZ to plot in the tholeiitic field. However, the second sample from this group (locality 8) plots within the calc-alkaline field due to a higher alkali component and a lower MgO concentration. The majority of the metamafic rocks from the S-SBDZ follows the curve separating the calc-alkaline and the tholeiitic fields, but is situated immediately below this line. The only analysis from this group in the tholeiitic field is 124. Surprisingly, the group of metamafic rocks (localities 40, 41, 122 and 123), which is in the alkali basalt field on the AFM diagram, is situated just above the separating curve in the tholeiitic field. The sample from locality 3 has a similar composition as the majority of the metamafic rocks in regard to the FeO*(total) content but displays lower values of MgO and higher values of total alkali. Therefore this sample falls in the tholeiitic field.

All porphyritic metamafic rocks from the N-SBDZ (locality 12) and S-SBDZ (locality 139), gabbro and metagabbro of Rödeby massif are poor in alkalis but rich in MgO and FeO*. Therefore they are situated close to each other in the diagram and are tholeiitic in composition.

4.2.2 Harker bivariate diagrams

On the Harker bivariate diagrams, the N-SBDZ metamafic rocks form a defined, slightly scattered cluster due to their limited SiO_2 variation. The majority of the metamafic rocks in the N-SBDZ generally have high SiO_2 contents (52 to 57 %). In the TAS-diagram they plot in the fields of andesitic basalts and andesites. The metamafic rocks display clear decreasing trends

of TiO_2, FeO*, MgO and CaO plotted against SiO_2 (Fig. 17). Concentrations of Al_2O_3, MnO and P_2O_5 plotted versus SiO_2 do not show any distinct trends. Na_2O and K_2O increase with increasing SiO_2 and a distinguished cluster of N-SBDZ metamafic rocks can be seen in the total alkali versus SiO_2 diagram (Fig. 15). The total alkali versus FeO*+TiO_2+MgO diagram (Fig. 18) shows a clear trend; decreasing alkali with increasing FeO*+TiO_2+MgO. However, two samples (8 and 18) have significantly different contents of most of the major elements. They are the most basic (SiO_2 - 48.98 and 47.85 respectively) rocks within the N-SBDZ metamafic rocks and are higher in CaO and Al_2O_3 but lower in Na_2O, TiO_2, FeO* and MnO. These two rocks are considered as non-representative because they occur in a complex geological setting and are highly affected by the deformation along the SBDZ and by the emplacement of the younger Eringsboda granites (see field description).

There is only one chemical analysis of the porphyritic metamafic rocks from the N-SBDZ (locality 12) available. The analysis shows a SiO_2 concentration of 52 and high values of FeO*, MnO, MgO and CaO but low concentrations of Al_2O_3, K_2O and Na_2O compared to the other N-SBDZ metamafic rocks.

The metamafic rocks from the S-SBDZ are more scattered in their major element concentrations. There are at least three distinct groups of rocks within the S-SBDZ.

The calc- alkaline metamafic rocks (localities 32, 34, 35, 117-1, 117-2, 124, 140 and 142) plot in a separate cluster with SiO_2 contents ranging between 49 to 53%. Analyses of this rather uniform group show decreasing trends of FeO*, MgO, MnO and CaO versus silica. However, Al_2O_3, K_2O and P_2O_5 contents are almost constant showing no trends.

The trachyandesite from locality 3 has a very different chemical composition from the rest of the S-SBDZ metamafic rocks. It is significantly high in K_2O, SiO_2 and low in MgO, CaO. It also displays minor differences in the rest of the major elements compared to the other S-SBDZ metamafic rocks.

The group of tholeiitic metamafic rocks (localities 40, 41, 122 and 123) are the most basic ones among the S-SBDZ metamafic rocks (SiO_2 contents ranging from 45 to 47). They are clustering separately in most of the bivariate diagrams. They are relatively high in FeO* and low in alkali. However, one of the samples within this group has a very similar composition

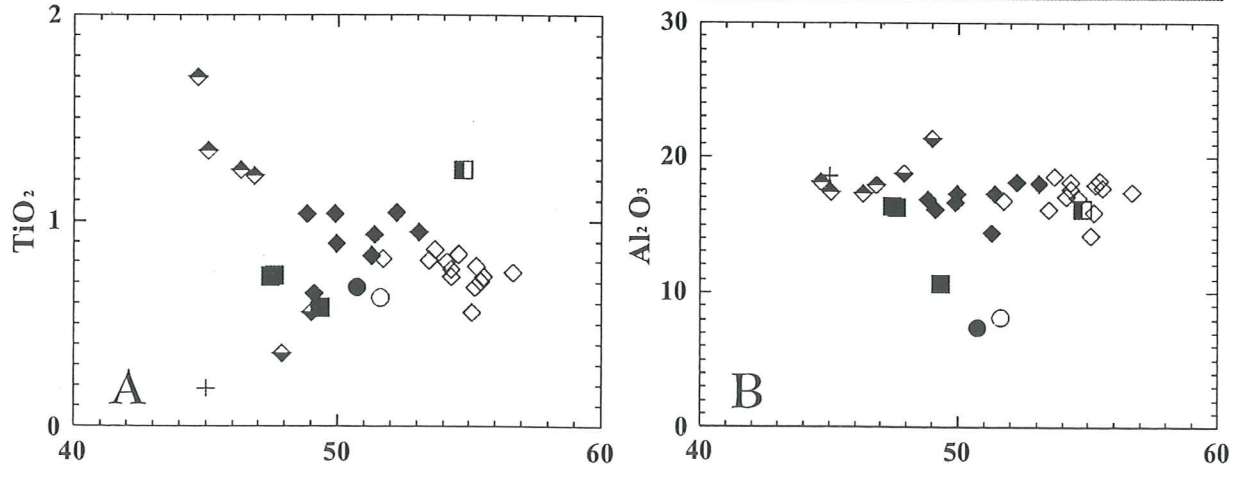

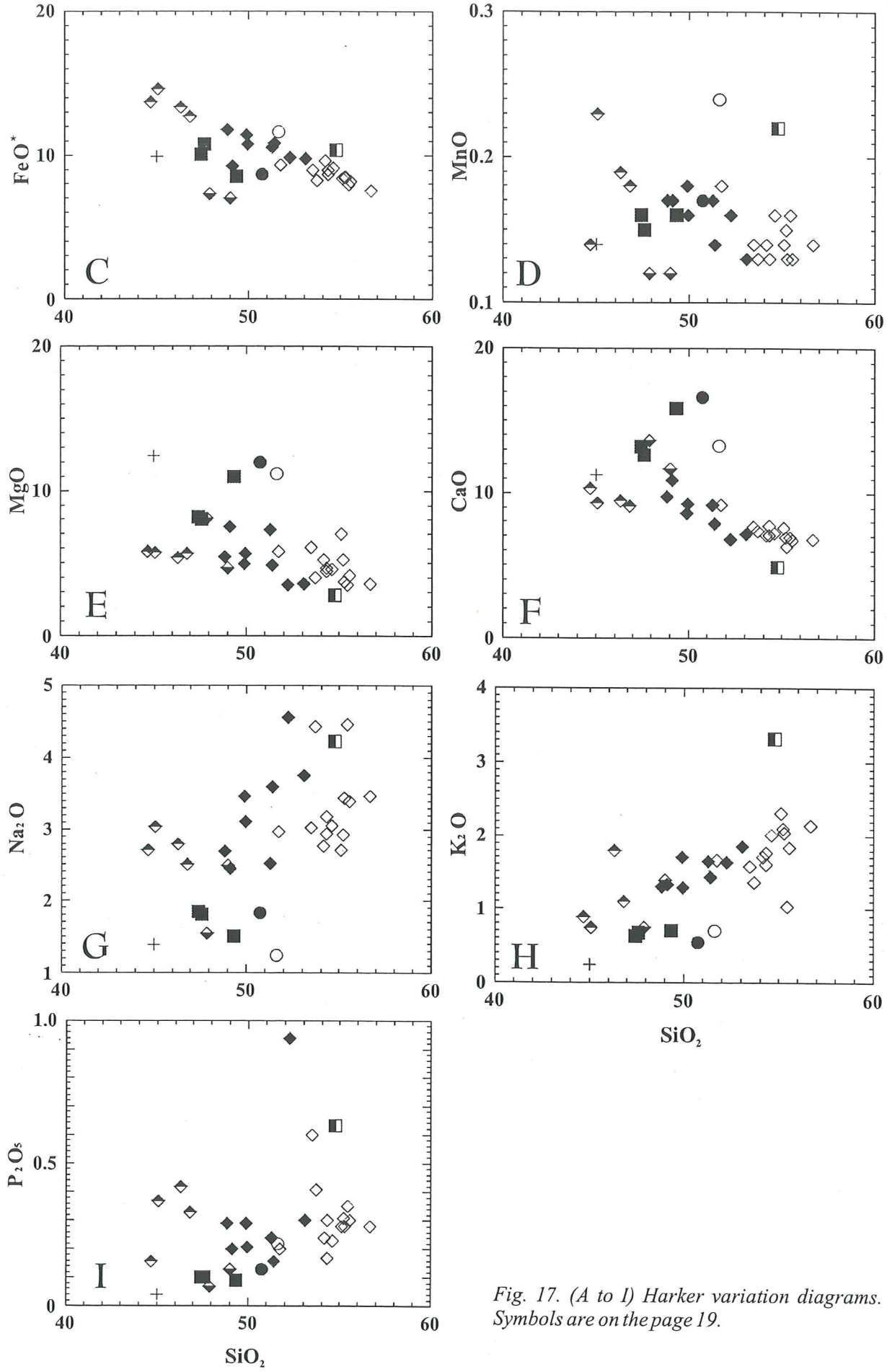

Fig. 17. (A to I) Harker variation diagrams. Symbols are on the page 19.

to the rest with exception of a higher TiO_2 value and lower values of MnO and P_2O_5 values

The porphyritic metamafic rocks from the S-SBDZ (locality 139) have many similarities to the N-SBDZ porphyritic metamafic rock. They differ however, by lower values of FeO* and MnO but a higher CaO value.

Two of the coarse- grained metagabbro have identical values of major, trace element and REE. They are more basic and significantly differ in Al_2O_3, MgO and CaO concentrations from other sample.

The olivine gabbro is very poor in TiO_2, P_2O_5 and alkali components but is, as expected from the mineral composition, rich in MgO.

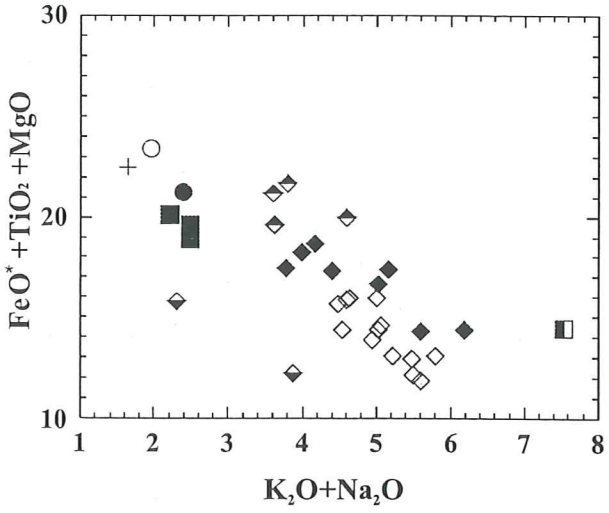

Fig. 18. FeO^*+TiO_2+MgO versus total alkalis diagram. Symbols are on the page 19.

4.3 Spiderdiagram

The trace element distribution of the metamafic rocks from both subprovinces is scattered. To define trends or clusters in Harker bivariate trace element diagrams proved impossible.

Trace elements of the mafic rocks have been normalized to the primordial mantle (Sun & McDonough, 1989; Fig. 19). In general, all rocks have a decreasing trend from the incompatible elements towards the compatible element. K, P and Ti show large negative anomalies for all samples. Trends are scattered but some similarities in the variation for the different rocks can be observed.

The metamafic rocks from the N-SBDZ have similar contents of trace elements (Fig. 19a,b) with strongly fractionated trends. A significant feature of these rocks is a strong negative anomaly of Nb and Ta. The group of the two samples (localities 8 and 18) displays a similar trend, but shows lower abundances of all elements. This group has similar negative anomalies of Nb and Ta. Additionally, the strong positive anomaly of Sr is common for both rocks of this group.

The S-SBDZ calc- alkaline metamafic rocks (Fig. 19c) exhibit a uniform variation of trace elements. Negative Nb and Ta anomalies are obvious. The trachyandesite from locality 3 has a very scattered trend with negative Th and Sr anomalies. Weaker negative Nb and Sm and positive Nd and Zr anomalies are present in this sample. The tholeiitic metamafic rocks (localities 40, 41, 122 and 123) are scattered. The highest variation is found in the concentration of Ba, Zr and Hf. Other trace elements have more or less similar values. There is a negative anomaly of Th, Nb and Ta for all the samples of this group.

The porphyritic metamafic rock from N-SBDZ (locality 12; Fig. 19b) also is scattered. Characteristic for this rock are high positive Th and La anomalies and negative anomalies of Nd, Sr and Zr. The S-SBDZ porphyritic metamafic rock (locality 139) is lower in most elements than the sample from locality 12, but trends are

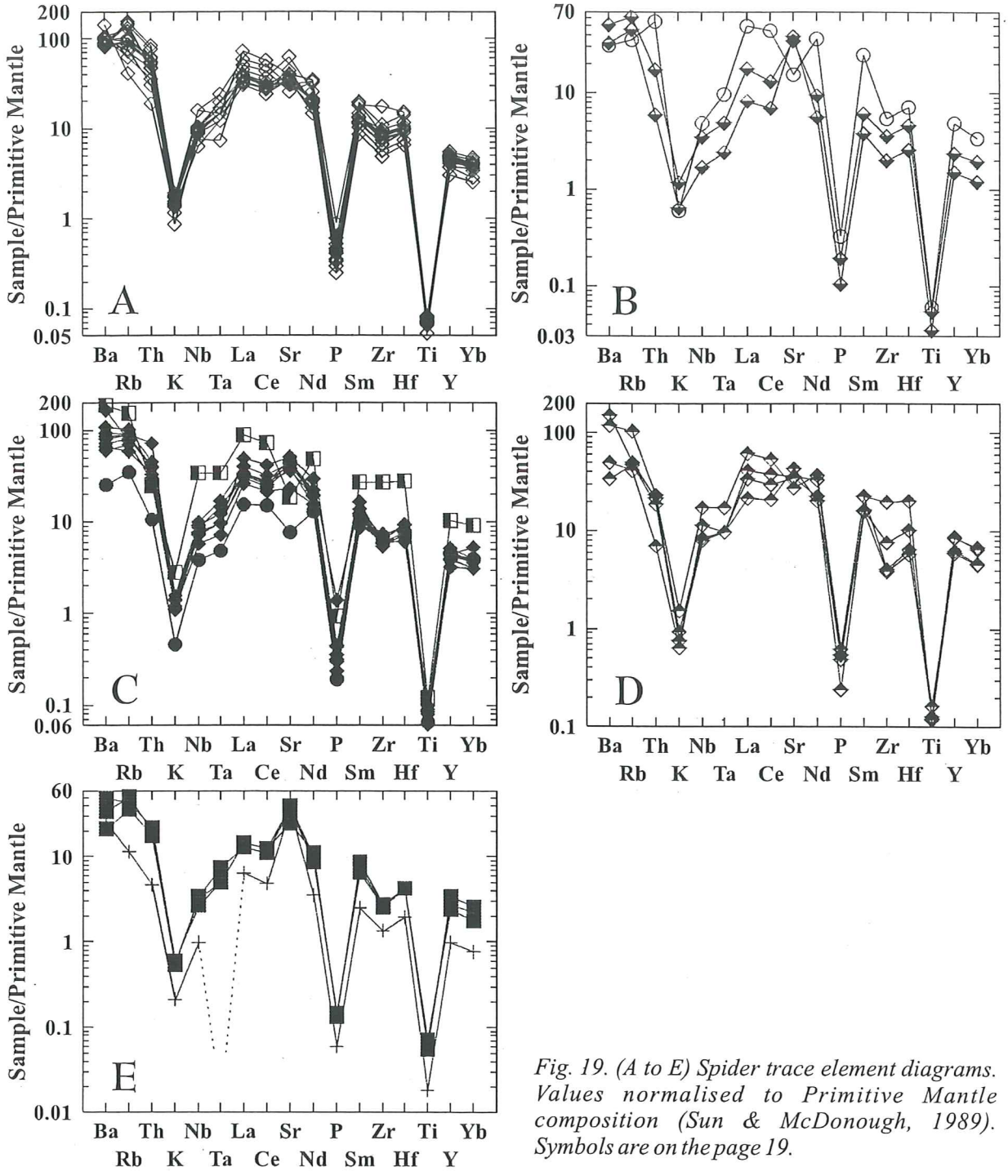

Fig. 19. (A to E) Spider trace element diagrams. Values normalised to Primitive Mantle composition (Sun & McDonough, 1989). Symbols are on the page 19.

rather similar. The exception is the lack of a positive Th anomaly for the sample from S-SBDZ (locality 139).

Samples of the S-SBDZ metagabbro (localities 38, 121 and 131) have similar concentrations of all the trace elements. The trends display a clear negative anomaly of Nb and a positive anomaly of Sr. A small negative anomaly of Zr is common as well. The olivine gabbro exhibits low values of most of the trace elements with clear positive anomalies of La and Sr and a negative anomaly for Nb.

4.4 REE pattern

The REE patterns are presented in Fig. 20. In general, all the rock types display similar LREE-enriched patterns.

The N-SBDZ metamafic rocks show a gradually decreasing trend with no Eu anomaly. One of the samples has weak positive anomalies of Tm and Lu. The group of two samples (localities 8 and 18) have in general similar trends compared to majority of the metamafic rocks from N-SBDZ but are lower in all REE s. A significant feature is a weak positive Eu anomaly.

The calc- alkaline metamafic rocks from the S-SBDZ have a gradually decreasing trend. A small positive anomaly of Yb appears in the trend for one of the samples. All the samples lack a Eu anomaly. Trachyandesite from locality 3 has a continuously decreasing trend from La to Gd. The HREE part of the trend from Gd is almost flat merely slightly decreasing from 40 to 30 times compare to the chondritic value. Neither this sample does have a Eu anomaly.

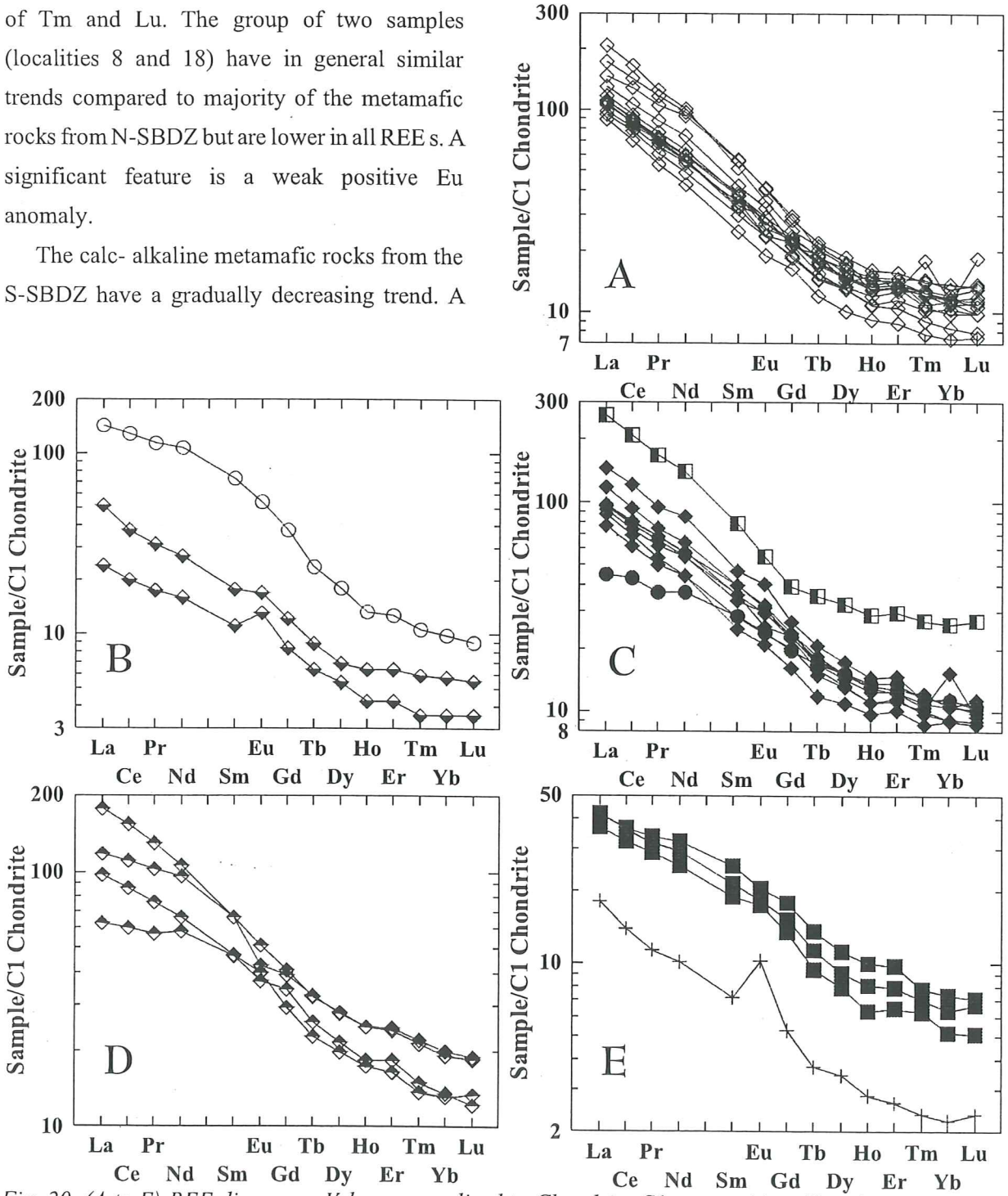

Fig. 20. (A to E) REE diagrams. Values normalised to Chondrite C1 composition (Sun & McDonough, 1989). Symbols are on the page 19.

The tholeiitic metamafic rocks (localities 40, 41, 122 and 123) have a scattered LREE patterns, but similar HREE trends. All the samples of this group lack a Eu anomaly as well as any other anomalies.

The porphyritic metamafic rock from the N-SBDZ (locality 12) has a strongly fractionated REE trend. No anomalies are present. The sample of the porphyritic metamafic rock from the S-SBDZ (locality 139) has a weakly fractionated trend. The HREE end is similar to the other metamafic rocks from the S-SBDZ. The REE trends of the metagabbro (localities 38, 121 and 131) have a low degree of fractionation with no Eu anomaly.

The olivine gabbro has the lowest value of all the REE within the rocks of this study. The concentration of La is about 10 times and Lu twice the chondritic value. It has a gradually decreasing trend with a positive Eu anomaly.

5. Overview of the results

When summarising the petrological data of the metamafic rocks, four major groups of rocks can be distinguished based on field observations, petrographic and geochemical data:

(1) The calc-alkaline metamafic rocks from the N-SBDZ;

The S-SBDZ:

(2) The calc-alkaline metamafic rocks;

(3) The tholeiitic metamafic rocks;

(4) The gabbro and metagabbro from the Rödeby massif.

The petrogenesis of these rock groups is discussed below in more details. In addition to these there are few minor groups.

The fine- to meddium-grained metamafic rocks found at localities 8 and 18 have a similar appearance as the majority of the fine-grained metamafic rocks from the N-SBDZ. However, this group has a strictly subalkaline basaltic composition on the TAS diagram (Fig. 15) but in the AFM diagram it splits into the calc- alkaline and tholeiitic fields. Neither field observation nor geochemical data help to unravel the relationship between the two groups of metamafic rocks. It is unclear whether the massif SW of Nävragöl is mainly composed of subalkaline basaltic rocks or this massif predominantly consists of calc-alkaline rock (majority group). Field observations show that both types of rocks are present in this massif.

The porphyritic metamafic rock from the N-SBDZ was collected from the massif SW of Nävragöl where several types of metamafic rocks appear (see field description). The field relationship between the different types of metamafic rocks in this massif is not clear and the limited number of geochemical analyses from this massif does not permit any conclusions about a possible relationship between the porphyritic and the fine-grained metamafic rock.

The porphyritic metamafic rock from the S-SBDZ comes from the massif on the Sturkö Island. It is related to the calc-alkaline fine-grained metamafic rocks typical for the S-SBDZ. The field relationships show that they are comagmatic with a gradual transition between the porphyritic and the fine-grained metamafic rocks. The sample of the porphyritic metamafic rock is slightly more basic and has almost twice the contents of MgO and CaO than the fine-grained metamafic rocks; i.e. it is more primitive than the others. The REE trend of the porphyritic metamafic rock is less fractionated than a non porphyritic ones. This suggests that the porphyritic metamafic rock constitutes a

cumulative or early-crystallized part of the massif and is probably derived from the same source.

The fine-grained mafic to intermediate rock at locality 3 near Tving is not marked on the map of Kornfält (in press), probably due to the small scale of the map. It differs in appearance from the rest of the metamafic rocks by its mineral composition and texture, being a typical volcanic rock. This locality occurs close to the dacitic volcanics to the west of Tving and consequently, it most likely belongs to them.

Each type of the minor rock group appears only at single localities. Thus, they are considered non-representative and are not included into the discussion.

IV. DISCUSSION

Varieties of the metamafic rocks across the SBDZ

The majority of **the fine-grained metamafic rocks from the N-SBDZ** are spread over a wide area; nevertheless they are similar in mineralogical and chemical composition. Variations in primary magmatic textures are depended on the emplacement situation, PT conditions and cooling rates. However, petrographic analyses showed that most of the rocks is metamorphosed and recrystallized; thus, the primary texture is erased and the secondary one is dependent on different degree of metamorphic overprint and deformation. On the TAS classification diagram (Fig. 15) this group falls in the basaltic andesite or andesite fields. On the AFM diagram (Fig. 16) they are strictly calc-alkaline.

The S-SBDZ fine-grained metamafic rocks form a group with similar textures and mineralogy, but the chemical composition allows to separate them into two major subgroups: (1) most of the metamafic rocks in the S-BSDZ are mainly basaltic composition (Fig. 15). They show a proper calc-alkaline trend on the AFM diagram, which is parallel to the trend of the metamafic rocks from N-SBDZ. (2)The second metamafic rock subgroup are more basic in composition with characteristically high values of TiO_2 and FeO* and slightly higher values of most trace elements than the first subgroup. They clearly differ from the calc-alkaline metamafic rocks of the S-SBDZ on the AFM diagram, being strictly tholeiitic (Fig. 16).

These two subgroups of the S-SBDZ metamafic rocks are somewhat distinct in isotopic compositions. Johansson and Larsen (1989) have presented whole-rock Sm-Nd isotope data on the calc-alkaline and tholeiitic metamafic rocks. Sample 85028 (Johansson and Larsen, 1989) comes from a small massif to the west of the road between Karlskrona and Rödeby. This massif is included in the tholeiitic metamafic subgroup. Sample 85029 (Johansson and Larsen, 1989) corresponds to sample 122 (this work) and sample 85030 (Johansson and Larsen, 1989) to sample 140 (this work). Johansson and Larsen (1989) calculated the initial ε_{Nd} value for T=1700 Ma. My field observation and geochemical data shows that mafic and enclosing rocks are of the same age (see the discussion below). Therefore, the initial ε_{Nd} value were recalculated for T=1770 Ma, which corresponds to the age of the Tving granitoids (Johansson and Larsen, 1989). The initial ε_{Nd} value shows a small difference

between samples of calc- alkaline and tholeiitic metamafic rocks. The ε_{Nd} value of +0.9 and +1.0 for the samples of tholeiitic metamafic rocks (samples 85028 and 85029 of Johansson and Larsen, 1989) and ε_{Nd} value of +1.7 for the calc- alkaline metamafic rock (sample 85030 of Johansson and Larsen, 1989) were obtained after recalculation. The authors did not separate these rocks into different subgroups on the base of the available Sm-Nd data.

The difference in ε_{Nd} values between two subgroups consider to be insignificant; i.e. indiates the same mantle source. Therefore, the geochemical data points towards the conclusion that the tholeiitic fine-grained metamafic rocks are more primitive member of the same rock suite as the calc-alkaline metamafic rocks. The geochemical differences, are most probably due to different degrees of crustal contamination and magmatic differentiation. The small massifs in between localities 41 and 123 are included in the same group of the tholeiitic metamafic rocks (Fig. 2).

It is questionable whether the variation of the major elements on Harker diagrams of **the olivine gabbro and metagabbro of the Rödeby massif** reflect magmatic evolution trends. The trace element and REE values are slightly higher for the metagabbroic rocks than for the olivine gabbro. The positive Eu anomaly for the olivine gabbro and absence of a Eu anomaly for the metagabbros suggest the fractional crystallization process due to accumulation of plagioclase into the olivine gabbro. The relationships between the fine-grained metamafic rocks and the gabbroids are unclear. The metamafic rocks (calc-alkaline and tholeiitic) hardly correlate by chemistry with the gabbroic rocks.

There are no age determinations or isotopic data for the Rödeby gabbroid massif. However, the petrography and geochemistry of the Rödeby gabbro are similar to the Rymmen gabbro, which is located 50 km NW of Växjö at the western boundary of the Småland-Värmland batholite within the Protogine Zone. The detailed petrological work on the Rymmen gabbro (Claeson, 1998) showed identical to Rödeby gabbro kelyphytic coronas and reaction rims between olivine and plagioclase. That implies a similar geochemistry of the magma and same PT parameters for the Rödeby and Rymmen mafic intrusions. The pressure estimated for the olivine-plagioclase reaction in literature shows a range of 6 to 10 kbar (Claeson, 1988; Griffin, 1971; Burns, 1985; Khan et al., 1989). The well-defined 1692±7 $^{207}Pb/^{206}Pb$ plateau age of the Rymmen gabbro (Claeson, 1999) is within the age span of 1.71 to 1.68 Ga for the surrounding Småland granitoids (Johansson 1990; Welin 1994; Wikman 1993, 1997). The observed mingling contacts between the Rymmen gabbro and the surrounding granitoids of the same age support the age determinations (Claeson 1999). The age relationship between the Rödeby gabbro and the enclosing Tving granitoids is unknown. I suggest, without any further prove, that the Rödeby gabbro and Tving granitoids are of the same age. If the assumption is correct, the comagmatic assemblage of gabbro and granitoids in both the Rymmen and Rödeby areas suggests a similar tectonic situation. In that case, the suggestion of Kornfält (2000) for the same igneous event for the Småland and Tving granitoids gets indirect support. However, the crystallization age of the Rödeby gabbro should be established before this hypothesis can be confirmed.

Petrogenetic relationships between the metamafic rocks across the SBDZ

The important question is whether any relationship exists between the metamafic rocks across the SBDZ. The separate clusters of the S- and N-SBDZ fine-grained metamafic rocks seem to occupy the opposite ends of the same, weakly defined trends on Harker diagrams (Fig. 17). The S-SBDZ tholeiitic and calc-alkaline metamafic rocks are in general more basic in character than the N-SBDZ calc-alkaline metamafic rocks; however, the trace element and REE trends are almost identical. The explanation might be different degrees of contamination of basic melts or contamination with different crustal material on both sides of the SBDZ. The major element data for the tholeiitic and calc-alkaline metamafic rocks across the SBDZ corroborate with the geochemical data presented by Lindh et al. (2001) for the Småland granitoids in the N-SBDZ and Tving granitoids in the S-SBDZ. The alternative or, most probably, an additional process, causing the geochemical variation, can be magmatic differentiation. However, is not well established because magmatic differentiation and contamination overlap each other in the sense of geochemical data and therefore, the separation of them becomes problematic. A single Sm-Nd analysis on the calc-alkaline metamafic rock from N-SBDS is available from the publication of Johansson and Larsen (1989). Sample 84095 of Johansson and Larsen (1989) is from the same locality as sample 25 of this work. On the base of the same reasons as for the S-SBDZ metamafic rocks the ε_{Nd} value were recalculated for T=1770 Ma (the age of the Tving granitoids). According to the unprecise available dating, the Småland granitoids should be at least 10 Ma older than Tving granitoids (Kornfält and Vaasjoki, 1999; Kornfält, 2000) but this difference in age is not very significant for the ε_{Nd} values. The increasing of age in 10 Ma increases the ε_{Nd} value with 0.1. The ε_{Nd} value of +1.0 for the T=1770 Ma obtained after recalculation, is in good agreement with the ε_{Nd} value for the tholeiitic (ε_{Nd} value +0.9 and +1.0) and calc-alkaline (ε_{Nd} value +1.7) metamafic rocks. It is difficult to correlate the metamafic rocks across the SBDZ because only one analysis from N-SBDZ is available. However, available Sm and Nd isotope data indicates no difference in the source rock for metamafic rocks across the SBDZ.

Mingling and mixing as a major age relationships indicator

The field relationships between metamafic rocks and granitoids at localities 30, 137 and 138 from N-SBDZ and localities 117 and 124 from the S-SBDZ indicate mingling and localised mixing between these two rock types. According to the definitions of Bacon (1986) and Sparks and Marshall (1986), mixed magmas that blended to form a homogeneous composition are termed 'mixed' or 'hybrid' magmas, whereas the term 'mingling' or 'co-mingling' is used if the magmas are mixed physically, but heterogeneities (like banding or enclaves/inclusions) are present in rock.

Field observation at locality 138 in the N-SBDZ showed that the fine- grained intermediate matrix contains phenocrysts of K-feldspar typical for the surrounding granitoids. The breccia from locality 117 shows in thin

sections that the fragments of the metamafic rock have incorporated xenocrysts of K-feldspar as well. K-feldspar is not common in the fragments of metamafic rocks, which have low K_2O concentration; and therefore the most probable explanation is that the K-feldspar was incorporated from the surrounding partly crystallised granitoids during the intrusion of the mafic magmas. Cooling time of the metamafic rock fragments was fairly short that is indicated by their fine-grained texture. Thus, the 'surviving' of the large crystals of K-feldspar in the potassium unsaturated melts remains a possibility.

The presence of intermediate, fine-grained rock in the matrix suggests localized mixing between the mafic and granitic magmas. According to Gençalioğlu Kuşcu and Floyd (2001) it is possible that the two end-member magmas did not mix thoroughly due to large temperature differences between the two magmas and the relatively small volume proportion of the mafic magma available. In order to test the localized mixing, a detailed

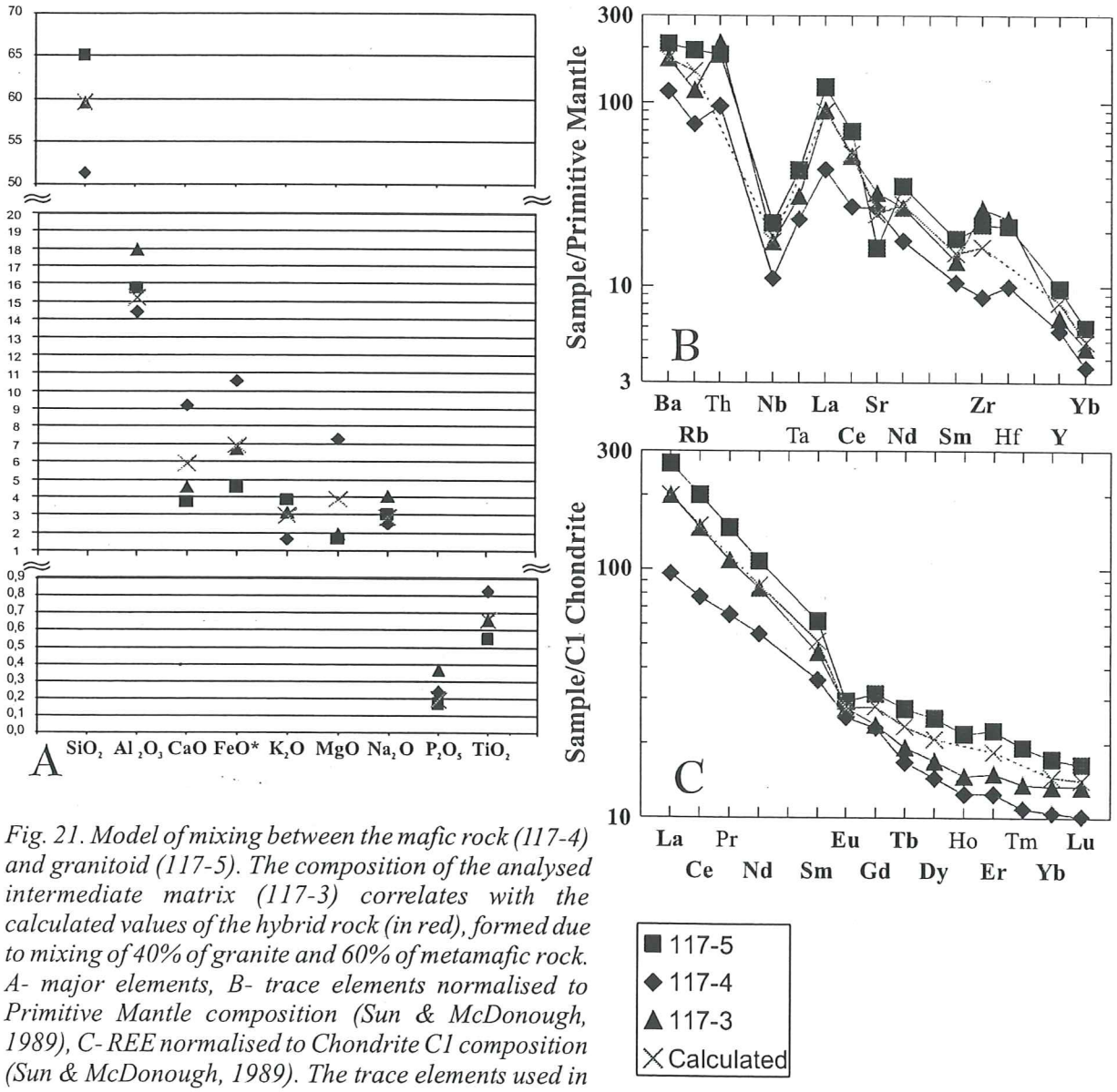

Fig. 21. Model of mixing between the mafic rock (117-4) and granitoid (117-5). The composition of the analysed intermediate matrix (117-3) correlates with the calculated values of the hybrid rock (in red), formed due to mixing of 40% of granite and 60% of metamafic rock. A- major elements, B- trace elements normalised to Primitive Mantle composition (Sun & McDonough, 1989), C- REE normalised to Chondrite C1 composition (Sun & McDonough, 1989). The trace elements used in the calculation for the diagrams B and C are in bold. ***Symbols are valid only for figure 21 A, B and C.***

geochemical study was performed on rocks from locality 117. The samples were collected from (1) the fine-grained metamafic rock (sample 117-4), (2) the intermediate, grey fine-grained matrix (sample 117-3) and (3) the enclosing coarse-grained granite (sample 117-5). All samples were analysed for major and trace elements including REE. A model for the mixing of the granite and the metamafic rock was constructed. The program Mistura 1.0 (Teixeira, 1996) was used. The theoretical composition of the mixed rock was compared with the composition of the fine- grain matrix for testing whether it is possible to obtain the rock of matrix composition through mixing of granitic and metamafic rocks as two end-members. The second task was to determine the exact amount of each component. The results of modelling are presented in the Table 12 and diagrams (Fig. 21).The geochemical data show that the fine-grained martix is enriched in few major elements (Al_2O_3, Na_2O and P_2O_5) and trace elements (Th, Sr, Zr and Hf) compare to the granitoid and metamafic rock. The rest of the major and trace elements including all the REE are within mixing range between the mafic and granitic end member. Calculated composition of the hybrid rock show that the grey intermediate rock in the matrix of the breccia at locality 117 is consistent with the hypothesis that it is a hybrid rock, which was formed due to mixing of 40% of granite and 60% of metamafic rock. Half of the major elements (SiO_2, FeO*, K_2O and TiO_2) and most of the trace elements used in the calculations (Ba, Nb, La, Nd, Sm, Yb and LREE) has identical values for the fine-grained rock in the matrix of the breccia and calculated hybrid rock. The rest of elements show simular but not identical values. The rock in the matrix of the breccia is also depleted in HREE (from Gd to Tm) compare to the calculated values. As the simplest explanation, the differences between the real geochemical data and calculated values of the hybrid rock, can be due to inhomogeneous or incomplete mixing between mafic rock and granitoid.

Thus the field observations and the geochemical model indicate mingling between the granitoids and metamafic rocks on either side of the SBDZ and prove a similar age for both rocks.

The P-T estimations gave a similar results for the metamafic rock and the intermediate matrix. The calculated pressure of 5 to 7 kbar and temperature of 600 to 870 °C for both rocks, most probably, do not indicates the crystallization, but element diffusion closure conditions, which can happend after the metamorphism. However, these unprecise P-T estimations can be used as indicator for erosion level in the S-SBDZ, which would be approximately 20-25 km.

Source of the metamafic rocks

Th/Ta and La/Yb ratios have been used to constrain possible sources for the mafic rocks of the studied area. The ratio of the incompatible elements (Th/Ta) has an advantage of minimizing the effect of fractional crystallization, partial melting and other magmatic processes and thus most likely to record source characteristics (Condie, 1997). La/Yb ratio is selected as a measure of the slope of the REE distribution.

Metamafic rocks from both sides of the SBDZ have similar values of the Th/Ta ratio (between 4 and 9) and La/Yb (between 10 and 25). Most of them fall between field of Arcs and

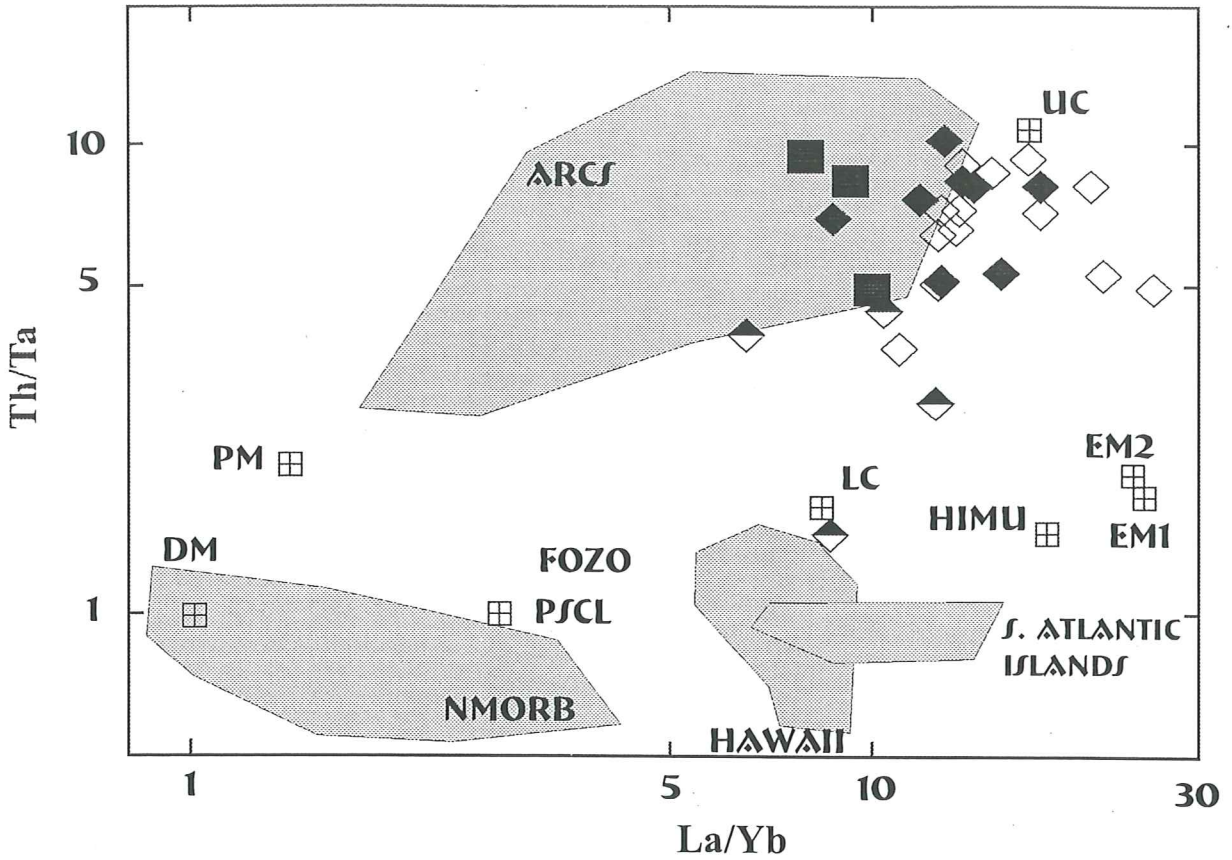

Fig. 22. Th/Ta versus La/Yb graph showing distribution of the basalts from various sources. DM, depleted mantle; PM, primitive mantle; PSCL, post-Archean subcontinental lithosphere; LC, lower continental crust; UC, upper continental crust; HIMU, high U/Pb mantle source; EM 1 and EM 2, enriched mantle source; FOZO, lower mantle plume component (area on the graph near and around the word FOZO). Data for tectonic settings from Condie (1997) and references cited therein. Symbols are on the page 19.

upper crust (UC) field (Fig. 22). The samples of the tholeiitic and few N-SBDZ calc-alkaline metamafic rocks have lower values of the ratio Th/Ta; therefore they are situated below the field of Arcs close to the composition of the lower crust (LC). The metagabbro have various Th/Ta and La/Yb ratios but fall strictly within the Arcs field. The sample of olivine gabbro has a value of Ta below the detection limit so it is not plotted on this diagram.

The diagram of Condie (1997) indicates a few possibilities to explain the source composition for the metamafic rocks across the SBDZ. One of the possibilities is that they had different mantle sources. However, keeping in mind that the metamafic rocks mingled with both Småland and Tving granitoids of similar approximately 1770- 1800 Ma age across the SBDZ, and there were not major horizontal movement along the SBDZ (Lindh et al., 2001), the probability of different mantle sources at the same place and at the same time is ambiguous.

Another explanation may be that the metamafic rocks were derived from the same mantle source but were contaminated to different degrees by rocks from the upper or lower continental crust. Following the discussion of Johansson and Larsen (1989), the initial ε_{Nd} values of the metamafic rocks across the SBDZ, as the simplest explanation, correspond to the same weakly depleted mantle source (ε_{Nd} ca. +1.5) at a time around 1770 Ma. However, a mixture of a more strongly depleted mantle source of (ε_{Nd} ca. +4) with pre-existing crustal materials (ε_{Nd} <0) are probable as well (Johansson and Larsen, 1989). To explain the

geochemical differences between the Småland granitoids in the N-SBDZ and the Tving granitoids in the S-SBDZ, Lindh et al. (2001) suggested different source rocks for the granitoids on either side of the SBDZ. The geochemical differences between the metamafic rocks across the SBDZ could be explained if one takes into account the suggestion of Johansson and Larsen (1989) that the source for the metamafic rocks across the SBDZ was a mixture of a more depleted mantle source and a pre-existing crust of different composition on either side of the SBDZ proposed by Lindh et al. (2001).

Tectonic setting of the metamafic rock formation

The petrogenetic diagrams based on the trace element composition have been used in order to obtain some information about possible tectonic settings of the studied mafic rocks. These diagrams have been constructed on base of a large set of data of mafic rocks from different modern tectonic settings (Rollinson, 1993). Application of these diagrams to old Proterozoic rocks does not necessarily reflect the precise tectonic position of their origin. This fact might be due to slightly different thermal regimes in the crust and mantle during Proterozoic times. Post-magmatic metamorphism of the rocks accompanied by metasomatic geochemical alteration must also be taken into account.

In two triangle diagrams Th-Hf/3-Ta (Fig. 22) and Th-Hf/3-Nb/16 (Fig. 23) most of the points from the different rock groups fall into the 'Destructive plate-margin basalt' field. However, one low-Th sample of the S-SBDZ tholeiitic metamafic rock falls into the 'E-MORB' and the 'WPB' field.

Enrichment in incompatible elements (e.g., Rb, Ba, Th) and negative Nb and Ta anomalies, typical for all the metamafic rocks across the SBDZ, are characteristic of a metasomatized mantle wedge source for subduction related basalts (Condie, 1997). This directly correlates with the results on the Th-Hf/3-Nb/16 or Ta diagram (Fig. 22 and 23) where most of the

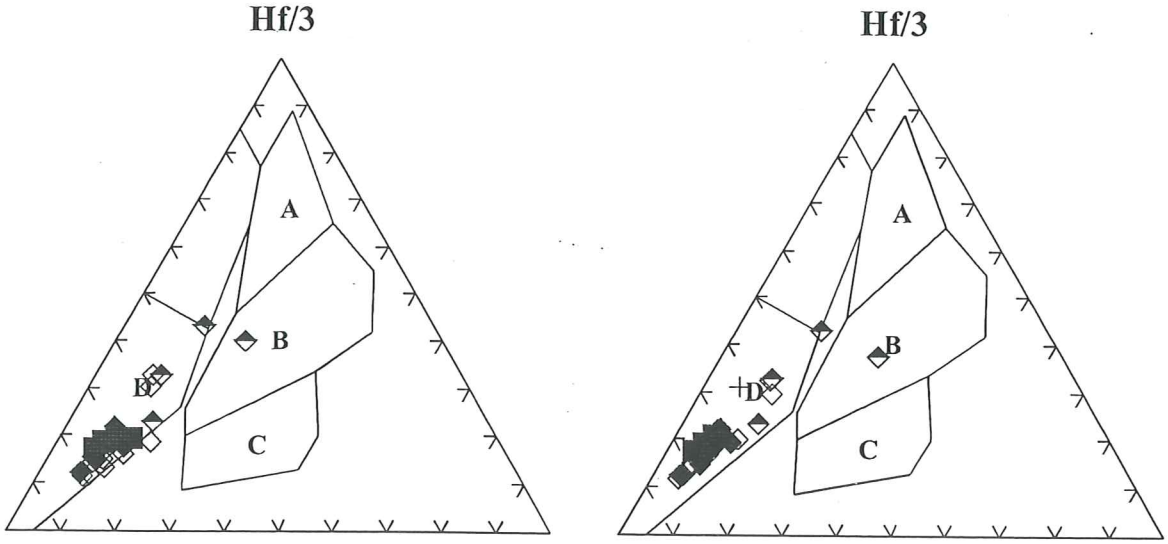

Fig. 23 and 24. Basalt discrimination diagrams (Wood, 1980). Field indexes: A- N-type MORB, B-E-type MORB and tholeiitic WPB (Within Plate Basalts), C-Alkaline WPB and WPB, D-Destructive plate-margin basalts. Symbols on the page 19.

samples fall into the field of 'Destructive plate-margin basalt'. My observations of the field relationships, petrographic analyses and geochemical model of mixing together with the isotopic data (Johansson and Larsen, 1989; Kornfält, 1993; Kornfält and Vaasjoki, 1996) suggest the same magmatic event for the mafic rocks and enclosing granitoids across the SBDZ. The tectonic setting of the TIB has been much debated although widely accepted opinion is convergent- margin environment due to subduction during an Andinotype orogeny (Wilson 1980; Nyström 1992; Andersson 1991; Gorbatschev & Bogdanova 1993). The trace element data and tectonic discrimination diagrams of the metamafic rocks, across the SBDZ, support this hypothesis.

V. CONCLUSIONS

1. As based on field relationships, petrography and geochemical characteristics, metamafic rocks across the Småland-Blekinge Deformation Zone (SBDZ) are classified into different groups composing separate massifs:

To the north of the SBDZ (the N-SBDZ subprovince) the majority of fine- grained metamafic rocks are strictly calc-alkaline, having a basalt-andesite or andesite composition. In contrast, to the south of the SBDZ (the S-SBDZ subprovince) two subgroups of the fine-grained metamafic rocks are distinguished. Both of them are basaltic composition, but one belonging to calc- alkaline series and another being tholeiitic.

The geochemical and isotopic data suggest that all the fine-grained metamafic rocks across the SBDZ belongs to the same rock suite. The geochemical differences are due to different degree of crustal contamination, magmatic differentiation of mafic melts and metamorphic overprint.

2. In the gabbroic Rödeby massif, the olivine gabbro is unmetamorphosed and undeformed, whereas the metagabbros probably represent intensely deformed and metamorphosed parts of this intrusion. The relationships to the fine-grained metamafic rocks are not established.

3. Field observations, petrography and geochemical modeling prove mingling and localized mixing between granitoids and mafic rocks. Therefore the fine-grained metamafic rocks across the SBDZ most probably are of the same age as Småland and Tving granitoids, i.e. 1770-1800 Ma.

4. Chemical and isotopic data suggest a uniform depleted mantle source for the mafic rocks and points toward the coherent terrane across the SBDZ at the time of the mafic intrusions. However, their major element variation suggests the contamination of the basic melts by a pre-existing crust of different composition on either side of the SBDZ.

5. The trace element variations of the studied metamafic rocks correspond to those in the destructive plate margin enviroment and support the hypothesis of the TIB formation in a convergent- margin environment due to an Andinotype orogeny.

Acknowledgements.- First, I want to thank my parents, sister and Ilka for love and support. My supervisors S. Bogdanova and A. Lindh share their time to discuss the questions, which rised like a cloud from the very beginning of this work. K.-A. Kornfält (SGU) kindly made his maps available to me before they were published and R. Gorbatschev for help during fieldworks and comments. Z. Solyom performed the major elements analyses and T. Miyazu helped with the SEM. I also want to thank A.Čečys and entire 'ex-jobarhuset' who rendered every kind of assistants. Lot of thanks to Ilka for comments, language corrections and access to the computer. Also would like to thank R. Kumpulainen (SU) for help with the Swedish abstract translation and comments. I acknowledge the Swedish Institute Visby programme for financial support.

Reference list

Andersson, U.B., 1991, Granitoid episodes and mafic-felsic magma interaction in the Svecofennian of the Fennoscandian shield, with main emphasis on the ca. 1.8 Ga plutonics: Precambrian Research, v. 51, p. 127-149.

Bacon, C.R., 1986, Magmatic inclusions in silicic and intermediate volcanic rocks: J. Geophysics. Res., v. 91, p. 6091-6112.

Blundy, J.D., Holland, T. J. B., 1990, Calcic amphibole equilibria and a new amphibole-plagioclase geothermometer: Contrib. Mineral Petrol, v. 104, p. 208-224.

Burns, L.E., 1985, The Border Ranges ultramafic and mafic complex, south-central Alaska: cumulate fractionates of island-arc volcanics: Canad. J. Earth Sci., v. 22, p. 1020-1038.

Claeson, D.T., 1998, Coronas, reaction rims, symplectites and emplacement depth of the Rymmen gabbro, Transscandinavian Igneous Belt, southern Sweden: Mineralogical Magazine, v. 62, p. 743-757.

Claeson, D.T., 1999, Geochronology of the Rymmen gabbro, southern Sweden; implication for primary versus inherited zircon in mafic rocks and rheomorphic dykes: GFF, v. 121, p. 25-31.

Condie, K.C., 1997, Sources of Proterozoic mafic dyke swarms: constraints from Th/Ta and La/Yb ratios: Precambrian Research, v. 81, p. 3-14.

Cox, K.G., Bell, J.D., Pankhurst, R.J., 1979, The interpretation of igneous rocks: London, George, Allen and Unwin.

Gaál, G., Gorbatschev, R., 1987, An outline of the Precambrian evolution of the Baltic Shield: Precambrian Research, v. 35, p. 15-52.

Geisler, T., Schleicher, H., 2000, Composition and U-Th-total Pb model ages of polygenetic zircons from the Vånga granite, south Sweden: an electron microprobe study: GFF, v. 122, p. 227-235.

Gençalioğlu Kuşcu, G., Floyd, P.A., 2001, Mineral composition and textural evidences for magma mingling in the Saraykent volcanics: Lithos, v. 56, p. 207-230.

Gorbatschev and bogdanova Gorbatschev, R., Bogdanova, S., 1993, Frontiers in the Baltic Shield: Precambrian Research, v. 64, p. 3-21.

Griffin, W.L., 1971, Genesis of Coronas in Anorthosites of the Upper Jotun Nappe, Indre Sogn, Norway: J. Petrol., v. 12, p. 219-243.

Hammarstrom, J.M., Zen, E-an., 1986, Aluminum in hornblende; an empirical igneous geobarometer: American Mineralogist, v. 71, p. 1297-1313.

Holland, T., Blundy, J., 1994, Non-ideal interactions in calcic amphiboles and their bearing on amphibole-plagioclase thermometry: Contrib. Mineral Petrol, v. 116, p. 433-447.

Hollister, L.S., Grissom, G.C., Peters, E.K., Stowell, H.H., Sisson, V.B., 1987, Confirmation of the empirical correlation of Al in hornblende with pressure of solidification of calc-alkaline plutons: American Mineralogist, v. 72, p. 231-239.

Irvine, T.N., Baragar, W. R. A., 1971, A guide to the chemical classification of the common volcanic rocks: Can. J. Earth Sci., v. 8, p. 523-548.

Johansson, Å., Larsen, O., 1989, Radiometric age determinations and Precambrian chronology of Blekinge, southern Sweden: GFF, v. 111, p. 35-50.

Johansson, Å. 1990, Age of the Önnestad syenite and some gneissic granites along the southern part of the Protogine Zone, southern Sweden: In C.F. Gower, T. Rivers & B. Ryan (ed.): Mid-Proterozoic Laurentia-Baltica. Geological Association of Canada, Special Paper 38, p. 131-148.

Johnson, M.C., Rutherford, M.J., 1989, Experimental calibration of an aliuminium-in-horblende geobarometer applicable to calc-alkaline rocks: Geology, v. 17, p. 837-841.

Khan, M.A., Jan, M.Q., Windley, B.F., Tarney, J., Thirlwall, M.F., 1989, The Chilas Mafic-Ultramafic Igneous Complex; The root of the Kohistan Island Arc in Himalayas of northern Pakistan: Geol. Soc. Amer. Special Paper, v. 232, p. 75-94.

Kornfält, K.-A., 1993, U-Pb zircon ages of three granite samples from Blekinge country, south-east Sweden: In T.Lundqvist (ed.): Radiometric dating results. SGU, v. C823, p. 17-23.

Kornfält, K.-A., 1996, U-Pb zircon ages of six granite samples from Blekinge country, south-east Sweden: In T.Lundqvist (ed.): Radiometric dating results2. SGU, v. C828, p. 15-31.

Kornfält, K.-A., 2000, Beskrivning till berggrundskartan 3F Karlskrona NO, SGU, v.Af199, p. 1-73.

Kornfält, K.-A., (In press), Berggrundskartan 3F Karlskrona NO (1:50 000), SGU, v.Af199.

Kornfält, K.-A., Bergström, J., 1990, Provisoriska översiktliga bergrundskarta. Bergrundskartan Karlskrona (1:250 000), SGU, v. Ba 44.

Kornfält, K.-A., Vaasjoki, M., 1999, U-Pb zircon datings of Småland and Karlshamn granites from southeasternmost Sweden: In S.Bergman (ed.): Radiometric dating results 4. SGU, v. C831, p. 32-41.

Leake, B.E., Woolley, A.R., Arps, C.E.S., Birch, W.D., Gilbert, M.C., Grice, J.D., Hawthorne, F.C., Kato, A., Kisch, H.J., Krivovichev, V.G., Linthout, K., Laird, J., Mandarino, J.A., Maresch, W.V., Nickel, E.H., Rock, N.M.S., Schumacher, J.C., Smith, D.C., Stephenson, N.C.N., Ungaretti, L., Whittaker, E.J.W., and Guo, Y., 1997, Nomenclature of amphiboles; report of the subcommittee on amphiboles of the International Mineralogical Association, Commission on New Minerals and Mineral Names: The Canadian Mineralogist, v. 9, p. 623-651.

Le Maître, R.W., Bateman, R., Dudek, A., Keller, J., Lameyre Le Bas, M.J., Sabine, P.A., Schmid, R., Sorensen, H., Streckeisen, A., Wolley, A.R., Zanettin, B., 1989, A classification of igneous rocks and glossary of terms: Oxford, Blackwell.

Lindh, A., Krauss, M., Franz, K.-M., 2001, Interpreting the Småland- Blekinge Deformation Zone from chemical and structural data: GFF, v. 123, p. 181-191.

MacDonald, G.A., Katsutra, T., 1964, Chemical composition of Hawaiian lavas: J. Petrology, v. 5, p. 83-133.

Nyström, J.O., 1982, Post-Svecokarelian Andinotype evolution in central Sweden: Geologische Rundschau, v. 71, p. 141-157.

Rickwood, P.C., 1989, Boundary lines within petrologic diagrams, which use oxides of major and minor elements: Lithos, v. 22, p. 247-263.

Rock, N.M.S., Carroll, G.W., 1990, MINTAB; a general-purpose mineral recalculation and tabulation program for Macintosh microcomputers: American Mineralogist, v. 75; 3-4, p. 424-430.

Rollinson, H.R., 1993, Using geochemical data: evaluation, presentation, interpretation: Harlow, Longman Group UK Limited.

Schmidt, M.W., 1992, Amphibole composition in tonalite as a function of pressure: an experimental calibration of the Al-in-hornblende barometer: Contrib. Mineral. Petrol., v. 110, p. 304-310.

Sparks, R.S.J., Marshall, L.A., 1986, Thermal and mechanical constraints on mixing between mafic and silicic magma: J. Volcanol. Geother. Res., v. 29, p. 99-124.

Sun, S., McDonough, W.F., 1989, Chemical and isotopic systematics of oceanic basalt: implication for the mantle composition and processes: Geol. Soc. London Spec. Publ., v. 42, p. 313-345.

Teixeira, L.R., 1996, Programme Genesis 1.1: O complexo Caraibae a suite Sao Jose do Jacuipe no Ciuturao Movel Salvador- Curaca (BA, Brasil): petrologia, geoquimica e potencial metalogenetico. Atese de dontarado intitulada.

Tindle, A.G., Webb, P.C., 1994, PROBE-AMPH- a spreadsheet program to classify microprobe-derived amphibole analyses: Computers & Geoscience, v. 20, p. 1201-1228.

Welin, E., Gorbatschev, R., and Kähr, A.-M., 1982, Zircon dating of polymetamorphic rocks in southwestern Sweden: Uppsala Stockholm, SGU ;Liber Kartor, 34 p.

Wiklander, U., 1974, Precambrian geology, geochemistry and age relationships of northeastern Blekinge, southern Sweden: SGU, v. C704, p. 3-142.

Wikman, H., 1993, U-Pb ages of the Småland granites and Småland volcanite from the Växjö region, southern Sweden: In T.Lundqvist (ed.): Radiometric dating results. SGU, v. C823, p. 65-72.

Wikman, H., 1997, U-Pb zircon ages of three granitoids from the Växjö region south central Sweden: In T.Lundqvist (ed.): Radiometric dating results 3. SGU, v. C830, p. 63-72.

Wood, D.A., 1980, The application of a Th-Hf-Ta diagram to problems of tectonomagmatic classification and to establishing the nature of crustal contamination of basaltic lavas of the British Tertiary volcanic province: Earth and Planetary Science Letters, v. 50; 1, p. 11-30.

Appendix

Locality	Rock type	Coordinates		Magnetic susceptibility in nTl	
		Long. E	Lat. N	Metamafic rock	Granitoid
N-SBDZ					
8	f- to m/gr metamafic rock	1482710	6247878	60	
12	porphyritic metamafic rock	1482712	6247836	n.m.	
18	f- to m/gr metamafic rock	1483781	6248397	50	
22	f/gr metamafic rock	1487140	6246898	50	
25	f/gr metamafic rock	1490137	6248188	4000	
26	f/gr metamafic rock	1491043	6247209	n.m.	
126	f/gr metamafic rock	1486920	6246891	60-90	
127	f/gr metamafic rock	1489982	6247829	4000	
128	f/gr metamafic rock	1490062	6249849	4000	
130	f/gr metamafic rock	1491683	6248565	3000-4000	
133	f/gr metamafic rock	1494545	6249673	1000-2000	
134	f/gr metamafic rock	1493925	6249833	50-2000	
135	f/gr metamafic rock	1485140	6258025	5000-4000	
136	f/gr metamafic rock	1494690	6258016	50	
137	f/gr metamafic rock	1495993	6258684	5000	
138	f/gr metamafic rock	1503362	6255936	2000-4000	
S-SBDZ					
3	f/gr metamafic rock	1480060	6242913	n.m.	
32	f/gr metamafic rock	1483372	6231797	50	
34	f/gr metamafic rock	1485318	6229171	1500-2000	1500-2000
35	f/gr metamafic rock	1484389	6229561	100-700	1500-2000
38	metagabbro	1486640	6234370	60-90	
39	olivine gabbro	1487237	6235557	500	
40	f/gr metamafic rock	1485870	6235294	50-3000	
41	f/gr metamafic rock	1483987	6235242	n.m.	
117	f/gr metamafic rock	1485973	6243732	100-200	2000
121	metagabbro	1486765	6235262	50-80	2000-3000
122	f/gr metamafic rock	1493066	6233562	3000	3000
123	f/gr metamafic rock	1493816	6233986	3000	
124	f/gr metamafic rock	1487044	6243449	200	2000
131	metagabbro	1484330	6236899	50-200-3000	
139	porphyritic metamafic rock	1495338	6220883	50	
140	f/gr metamafic rock	1495227	6220748	4000	600-1000
142	f/gr metamafic rock	1495809	6222339	5000-6000	

Table 1. List of the studied samples with outcrop coordinates (the Swedish grid with the RT90 coordinates system) and magnetic susceptibility measurements. F/gr fine-grained rock, m/gr medium-grained rock, n.m. not measured.

Thin section		Plag	Biotite	Amph	OPx	CPx	Opaque	Titanite	Apatite	Epidote	K-Fsp	Qtz
N-SBDZ												
8	f-m grained	54	+	43			+	2	+	1		
18	f-m grained	55		42			+		+	3		
22	f-grained	28	5	48			+	1	+		8	10
25	f-grained	22	+	65			+	1	+			12
26	f-grained	43	21	17			+		+			18
126	f-grained	39	13	36			+		+		+	12
127	f-grained	45	17	33			2		+			3
128	f-grained	53	20	15			1		+	10		3
130	f-grained	62	8	25			1		+	0		4
133	f-grained	44	11	31			1		+	4		8
135	f-grained	61	5	31			3		+			
136	f-grained	37	19	28			+	1	+	11		3
138	f-grained	50	19	15			1	2	+	13		1
12	porphyritic	16		72		+	+		+			12
S-SBDZ												
3	f-grained	17	22	20			3	5	+		4	29
32	f-grained	48	21	16			1	3	+			11
34	f-grained	32	13	50			+	3	+			2
35	f-grained	36	9	50			+	2	+			3
124	f-grained	34	13	47			1	4	+			
140	f-grained	56	10	31			2	1	+			
40	f-grained	44		54			2	+	+			
41	f-grained	38	7	48			1	1	+			4
122	f-grained	43	9	43			5		+			
123	f-grained	48	16	33			3		+			
38	metagabbro	36		61	1		1	1	+			
121	metagabbro	21	2	55		21	1		+			
131	metagabbro	36		59		5	+		+			
							+					
117-2	fragment	39	7	48			+	1	+	1	4	
117-3	martix	59	18	2			3	2	+		5	11

		Plag	Phlog	Amph	OPx	CPx	Ol	Opaque	Apatite	Amph-spinel simplectite		
39	Ol-gabbro	45	1	14	9	10	11	+	+	12		

(+) minerals present in very small amounts

Table 2. Modal compositions of the studied metamafic rocks. Point counting results (500 points on each thin section).

	Megacrysts							Matrix			
Sample number	12a-16	12a-21	12a-28	12a-34	12a-35	12a-37	12a-38	12a-44m	12a-49m	12a-51m	12a-53m
SiO_2	47.9	48.69	48.68	51.64	48.74	48.93	48.64	46.56	49.35	50.9	50.8
TiO_2	0.27	0.31	0.27	0.2	0.22	0.22	0.19	0.44	0.22	0.2	0.2
Al_2O_3	7.42	6.72	6.52	4.14	6.68	6.29	6.54	7.93	6.22	5.14	4.8
FeO*	13.9	12.93	13.53	11.75	13.66	13.63	13.61	14.8	13.88	13.03	12.62
MnO	0.27	0.33	0.34	0.22	0.3	0.25	0.33	0.37	0.34	0.16	0.36
MgO	13.09	13.86	13.69	15.51	13.52	13.8	13.56	12.14	13.73	14.26	14.49
CaO	12.97	12.98	13.07	13.45	13.16	13.04	12.93	12.84	13.18	13.22	13.3
Na_2O	0.8	0.76	0.69	0.46	0.56	0.59	0.75	0.86	0.61	0.52	0.46
K_2O	0.67	0.57	0.52	0.2	0.52	0.46	0.52	0.75	0.46	0.35	0.33
Total	97.29	97.15	97.31	97.57	97.36	97.21	97.07	96.69	97.99	97.78	97.36
Oxygen number	23	23	23	23	23	23	23	23	23	23	23
Si	7.06	7.14	7.14	7.47	7.15	7.17	7.16	6.96	7.19	7.39	7.41
Al iv	0.94	0.86	0.86	0.53	0.85	0.83	0.84	1.04	0.81	0.61	0.59
Al vi	0.35	0.31	0.27	0.17	0.31	0.26	0.29	0.35	0.26	0.27	0.23
Ti	0.03	0.03	0.03	0.02	0.02	0.02	0.02	0.05	0.02	0.02	0.02
Fe3+	0.08	0.08	0.12	0.00	0.10	0.17	0.13	0.09	0.13	0.00	0.00
Fe2+	1.63	1.51	1.54	1.42	1.57	1.50	1.55	1.76	1.56	1.58	1.54
Mn	0.03	0.04	0.04	0.03	0.04	0.03	0.04	0.05	0.04	0.02	0.04
Mg	2.88	3.03	3.00	3.34	2.96	3.02	2.97	2.70	2.98	3.09	3.15
Ca	2.05	2.04	2.06	2.08	2.07	2.05	2.04	2.06	2.06	2.06	2.08
Na	0.23	0.22	0.20	0.13	0.16	0.17	0.21	0.25	0.17	0.15	0.13
K	0.13	0.11	0.10	0.04	0.10	0.09	0.10	0.14	0.09	0.06	0.06
(Ca+Na) (B)	2.05	2.04	2.06	2.08	2.07	2.05	2.04	2.06	2.06	2.06	2.08
Na (B)	0.00	0.00	0.00	0.00	0.00	0.00	0.00	0.00	0.00	0.00	0.00
(Na+K) (A)	0.35	0.32	0.29	0.17	0.26	0.25	0.31	0.39	0.26	0.21	0.19
Mg/(Mg+Fe2)	0.64	0.67	0.66	0.70	0.65	0.67	0.66	0.61	0.66	0.66	0.67
Fe3/(Fe3+Alvi)	0.19	0.20	0.31	0.00	0.25	0.40	0.30	0.21	0.33	0.00	0.00
Amphibole name	magnesio-hornblende	magnesio-hornblende	magnesio-hornblende	actinolitic-hornblende	magnesio-hornblende	magnesio-hornblende	magnesio-hornblende	magnesio-hornblende	magnesio-hornblende	actinolitic-hornblende	actinolitic-hornblende

Table 3. Representative amphibole microprobe analyses from the N-SBDZ porphyritic metamafic rock. The program PROBE-AMPH (Tindle and Webb, 1994) was used to determine structural formula and mineral name.

	Inclusions in megacrysts				Matrix		
Sample	12a-14	12a-31	12a-36	12a-46	12a-50	12a-52	12a-55
Mineral	Plag	Plag	Plag	Plag	Plag	Plag	Plag
Na_2O	9.36	5.6	5.24	8.71	6.32	5.83	5.77
SiO_2	64.67	55.44	54.73	64.59	57.43	56.38	56.45
K_2O	0.06	0.13	0.07	0.81	0.11	0.15	0.11
FeO*	0.4	0.44	0.33	0.38	0.2	0.12	0.17
Al_2O_3	22	28.36	28.47	22.17	26.8	27.75	27.83
CaO	2.75	10.06	10.6	1.78	8.57	9.42	9.47
F	0.53	0.47	0.28	1	1.3	0.7	0.02
CalcTotal	99.77	100.5	99.72	99.44	100.73	100.35	99.82
OxNum	8	8	8	8	8	8	8
Si	2.85	2.49	2.47	2.85	2.56	2.52	2.54
Al	1.14	1.50	1.52	1.15	1.41	1.46	1.47
Fe*	0.02	0.02	0.01	0.01	0.01	0.01	0.01
Ca	0.13	0.48	0.51	0.08	0.41	0.45	0.46
Na	0.80	0.49	0.46	0.75	0.55	0.51	0.50
K	0.00	0.01	0.00	0.05	0.01	0.01	0.01
F	0.07	0.07	0.04	0.14	0.18	0.10	0.00
Albite	86	50	47	85	57	52	52
Anorthite	14	49	53	10	43	47	47
Orthoclase	0	1	0	5	1	1	1

Sample	12a-40	12a-41	12a-45
Mineral	Cpx	Cpx	Cpx
Na_2O	0.3	0.25	0.19
MgO	13.04	13.43	12.54
SiO_2	52.63	52.9	52.4
K_2O	0.03	0	0.02
TiO_2	0.1	0.06	0.12
MnO	0.26	0.39	0.44
FeO*	7.96	7.48	8.49
Al_2O_3	0.81	0.78	0.84
CaO	25.34	25.32	24.84
F	0.16	0.23	0
CalcTotal	100.56	100.74	99.88
OxNum	6	6	6
Si	1.96	1.96	1.97
Al	0.04	0.03	0.04
Fe*	0.25	0.23	0.27
Mg	0.73	0.74	0.70
Ca	1.01	1.01	1.00
Na	0.02	0.02	0.01
K	0.00	0.00	0.00
Ti	0.00	0.00	0.00
Mn	0.01	0.01	0.01
F	0.02	0.03	0.00
mg	74.49	76.20	72.46
Total Cat	4.04	4.04	4.01
Enstatite	37	37	36
Ferrosilite	12	12	14
Wollastonite	51	51	51

Table 4. Representative plagioclase and clinopyroxene microprobe analyses from the N-SBDZ porphyritic metamafic rock. The program MINTAB (Rock and Carroll, 1990) was used to determine structural formula.

Sample	39a-15	39a-16	39a-47	39a2-22	39a2-24
Mineral	Plag	Plag	Plag	Plag	Plag
Na_2O	1.67	0.34	0.65	1.09	2.16
SiO_2	45.8	42.51	44.07	45.04	47.35
K_2O	0	0.05	0.02	0	0.05
Al_2O_3	34.4	36.44	36.67	35.76	33.95
CaO	17.73	20.01	19.73	18.95	17.09
F	0.25	0	0.69	n.m.	n.m.
CalcTotal	99.85	99.35	101.83	101.2	100.74
OxNum	8	8	8	8	8
Si	2.11	1.98	2.00	2.06	2.16
Al	1.87	2.00	1.96	1.93	1.83
Ca	0.88	1.00	0.96	0.93	0.84
Na	0.15	0.03	0.06	0.10	0.19
K	0.00	0.00	0.00	0.00	0.00
F	0.04	0.00	0.10		
Total Cat	5.04	5.02	5.08	5.02	5.02
Albite	15	3	6	9	19
Anorthite	85	97	94	91	81
Orthoclase	0	0	0	0	0

	39a-2	39a2-27
Mineral	Olivine	Olivine
MgO	31.41	32.89
SiO_2	36.75	37.07
MnO	0.43	0.4
FeO*	30.99	28.48
Al_2O_3	0.05	0.16
CaO	0.03	0.02
CalcTotal	99.66	99.22
OxNum	4	4
Si	1.00	1.00
Al	0.00	0.01
Fe*	0.71	0.64
Mg	1.28	1.33
Ca	0.00	0.00
Mn	0.01	0.01
mg	64.38	67.30
Total Cat	3.00	3.00

Sample	39a-5	39a-6	39a-25	39a-26
Mineral	Cpx	Cpx	Opx	Opx
Na_2O	0.28	0.19	0	0
MgO	15.85	16.22	25.56	25.68
SiO_2	52.38	52.78	54.19	54.32
K_2O	0	0	0.03	0
TiO_2	0.24	0.19	0.08	0
MnO	0.14	0.12	0.38	0.41
FeO*	4.85	5.01	17.64	17.8
Al_2O_3	2.14	1.79	2.09	1.81
CaO	23.52	22.7	0.19	0.14
CalcTotal	99.39	99.11	100.16	100.14
OxNum	6	6	6	6
Si	1.94	1.95	1.96	1.97
Al	0.09	0.08	0.09	0.08
Fe*	0.15	0.16	0.53	0.54
Mg	0.87	0.89	1.38	1.39
Ca	0.93	0.90	0.01	0.01
Na	0.02	0.01	0.00	0.00
K	0.00	0.00	0.00	0.00
Ti	0.01	0.01	0.00	0.00
Mn	0.00	0.00	0.01	0.01
mg	85.34	85.22	72.09	72.01
Total Cat	4.02	4.02	3.99	3.99
Enstatite	45	46	72	72
Ferrosilite	8	8	28	28
Wollastonite	48	46	0	0

	39a-21	39a-43
Mineral	Spinel	Spinel
Na_2O	0.12	0.11
MgO	12.25	11.82
SiO_2	0.01	0.04
K_2O	0.04	0
TiO_2	0.08	0.01
MnO	0.12	0.14
FeO*	25.69	25.49
Al_2O_3	61.91	62.12
CaO	0.05	0.15
CalcTotal	100.31	99.93
OxNum	32	32
Si	0.00	0.01
Al	15.60	15.69
Fe*	4.59	4.57
Mg	3.90	3.77
Ca	0.01	0.04
Na	0.05	0.04
K	0.01	0.00
Ti	0.01	0.00
Mn	0.02	0.03
mg	45.94	45.25
Total Cat	24.20	24.14

	39a2-16	39a2-20
Mineral	Phlog	Phlog
Na_2O	0.93	0.98
MgO	20.1	20.31
SiO_2	37.35	38.04
K_2O	8.16	8.22
TiO_2	0.49	0.46
MnO	0	0.02
FeO	7.52	7.62
Al_2O_3	18.95	19.35
CaO	0.04	0.06
CalcTotal	93.54	95.06
OxNum	22	22
Si	5.43	5.44
Al	3.25	3.26
Fe*	0.91	0.91
Mg	4.36	4.33
Ca	0.01	0.01
Na	0.26	0.27
K	1.51	1.50
Ti	0.05	0.05
Mn	0.00	0.00
mg	82.65	82.61
Total Cat	15.78	15.77

Table 5. Representative microprobe analyses of major minerals from the olivine gabbro of the Rödeby massif. The program MINTAB (Rock and Carroll, 1990) was used to determine structural formula.

Amph. between:	Ol-Cpx		Pl-Cpx		Ol-Pl (Kelythytic coronas)						
Sample number	39a-3	39a-8	39a-17	39a-18	39a-22	39a-24	39a-40	39a-41	39a-42	39a-44	39a-52
SiO_2	53.72	52.6	44.57	42.63	43.49	44.13	44.14	45.45	44.23	43.95	47.87
TiO_2	0.22	0.28	0.7	0.9	0.14	0.14	0.13	0.27	0.16	0.19	0.2
Al_2O_3	3.58	3.8	12.35	14.39	14.89	14.39	14.07	12.06	13.98	15.05	10.86
FeO*	6.16	6.43	8.67	9.46	9.59	9.36	9.28	9.4	9.33	9.56	8.93
MnO	0.14	0.09	0.08	0.22	0.14	0.11	0.1	0.05	0.14	0.21	0.11
MgO	19.8	19.19	14.66	13.61	14.74	15.25	15.08	15.99	14.98	14.55	15.5
CaO	13.21	13.04	12.8	12.76	12.44	12.34	12.53	12.23	12.47	12.48	12.65
Na_2O	0.68	0.51	1.76	2	2.14	2.19	1.9	1.84	2.05	1.98	1.18
K_2O	0.01	0	0.09	0.12	0.29	0.31	0.19	0.17	0.17	0.21	0.1
Sum	97.52	95.94	95.68	96.09	97.86	98.22	97.42	97.46	97.51	98.18	97.4
Oxygen number	23	23	23	23	23	23	23	23	23	23	23
Si	7.52	7.49	6.52	6.25	6.20	6.25	6.30	6.45	6.31	6.23	6.80
Al iv	0.48	0.51	1.48	1.75	1.80	1.75	1.70	1.55	1.69	1.77	1.20
Al vi	0.11	0.12	0.65	0.74	0.70	0.65	0.66	0.47	0.66	0.75	0.62
Ti	0.02	0.03	0.08	0.10	0.02	0.01	0.01	0.03	0.02	0.02	0.02
Fe3+	0.18	0.21	0.14	0.21	0.64	0.68	0.63	0.77	0.58	0.61	0.34
Fe2+	0.54	0.55	0.92	0.95	0.50	0.43	0.48	0.35	0.54	0.52	0.72
Mn	0.02	0.01	0.01	0.03	0.02	0.01	0.01	0.01	0.02	0.03	0.01
Mg	4.13	4.07	3.20	2.98	3.13	3.22	3.21	3.38	3.19	3.08	3.28
Ca	1.98	1.99	2.01	2.00	1.90	1.87	1.91	1.86	1.91	1.90	1.93
Na	0.18	0.14	0.50	0.57	0.59	0.60	0.53	0.51	0.57	0.54	0.33
K	0.00	0.00	0.02	0.02	0.05	0.06	0.03	0.03	0.03	0.04	0.02
(Ca+Na) (B)	2.00	2.00	2.01	2.00	2.00	2.00	2.00	2.00	2.00	2.00	2.00
Na (B)	0.02	0.01	0.00	0.00	0.10	0.13	0.09	0.14	0.09	0.10	0.07
(Na+K) (A)	0.17	0.13	0.52	0.59	0.54	0.53	0.47	0.40	0.51	0.48	0.27
Mg/(Mg+Fe2)	0.88	0.88	0.78	0.76	0.86	0.88	0.87	0.91	0.86	0.85	0.82
Fe3/(Fe3+Alvi)	0.62	0.64	0.18	0.22	0.48	0.51	0.49	0.62	0.46	0.45	0.35
Amphibole names	actinolite	actinolitic hornblende	edenitic hornblende	pargasitic hornblende	pargasite	magnesio-hastingsite	tschermakitic hornblende	ferrian-tschermakitic hornblende	pargasitic hornblende	tschermakite	magnesio-hornblende

Table 6. Representative microprobe analyses of amphibole from reaction rims, Rödeby massif, olivine gabbro. The program PROBE-AMPH (Tindle and Webb, 1994) was used to determine structural formula and mineral name.

Sample number	40a1-13	40a1-14
SiO_2	44.40	44.28
TiO_2	0.90	0.93
Al_2O_3	9.46	9.43
FeO*	16.59	16.48
MnO	0.30	0.23
MgO	11.21	11.03
CaO	12.87	12.83
Na_2O	0.90	0.87
K_2O	0.98	1.02
Total	97.59	97.10
Oxygen number	23.00	23.00
Si	6.63	6.65
Al iv	1.37	1.35
Al vi	0.29	0.32
Ti	0.10	0.10
Fe3+	0.31	0.23
Fe2+	1.76	1.84
Mn	0.04	0.03
Mg	2.50	2.47
Ca	2.06	2.07
Na	0.26	0.25
K	0.19	0.20
Total	17.51	17.51
Amphibole group	Ca	Ca
(Ca+Na) (B)	2.06	2.07
Na (B)	0.00	0.00
(Na+K) (A)	0.45	0.45
Mg/(Mg+Fe2)	0.59	0.57
Fe3/(Fe3+Alvi)	0.51	0.42
Sum of S2	13	13
Amphibole names	magnesio-hornblende	magnesio-hornblende

Table 7. Representative amphibole microprobe analyses from the metagabbro of the Rödeby massif. The program PROBE-AMPH (Tindle and Webb, 1994) was used to determine structural formula and mineral name.

	Fragments						Martix	
Sample number	117a2-5	117a2-14	117a2-16	117a2-23	117a2-51	117a2-52	117a3-1	117a3-2
SiO_2	42.4	55.8	48.8	51.71	42.57	42.59	41.11	39.68
TiO_2	0.7	0.18	0.32	2.12	0.65	0.66	0.83	0.75
Al_2O_3	10.78	24.75	17.91	17.72	11.53	11.36	11.18	11.65
FeO*	20.5	1.87	12.09	7.68	19.6	19.75	21.22	21.52
MnO	0.32	0.09	0.12	0.09	0.37	0.31	0.78	0.79
MgO	8.58	0.68	4.49	3.03	8.2	8.08	7.64	7.07
CaO	12.36	6.76	9.41	8.95	13.12	13.19	12.19	11.78
Na_2O	1.12	6.09	3.75	3.67	1.21	1.24	1.04	1.01
K_2O	1.25	1.3	1.31	2.07	1.21	1.15	1.34	1.49
Total	98.01	97.52	98.2	97.04	98.46	98.33	97.33	95.74
Structural formula								
Oxygen number	23	23	23	23	23	23	23	23
Si	6.42	7.45	6.96	7.28	6.47	6.48	6.31	6.20
Al iv	1.58	0.55	1.04	0.72	1.53	1.52	1.69	1.80
Al vi	0.35	3.35	1.97	2.22	0.53	0.52	0.33	0.35
Ti	0.08	0.02	0.03	0.22	0.07	0.08	0.10	0.09
Fe3+	0.49	0.00	0.00	0.00	0.00	0.00	0.59	0.73
Fe2+	2.10	0.21	1.44	0.90	2.49	2.51	2.14	2.09
Mn	0.04	0.01	0.01	0.01	0.05	0.04	0.10	0.10
Mg	1.94	0.14	0.96	0.64	1.86	1.83	1.75	1.65
Ca	2.01	0.97	1.44	1.35	2.14	2.15	2.00	1.97
Na	0.33	1.58	1.04	1.00	0.36	0.37	0.31	0.31
K	0.24	0.22	0.24	0.37	0.23	0.22	0.26	0.30
Amphibole group	Ca	Na-Ca	Ca	Ca	Ca	Ca	Ca	Ca
(Ca+Na) (B)	2.01	2.00	2.00	2.00	2.14	2.15	2.00	2.00
Na (B)	0.00	1.03	0.56	0.65	0.00	0.00	0.00	0.03
(Na+K) (A)	0.57	0.77	0.71	0.72	0.59	0.59	0.57	0.58
Mg/(Mg+Fe2)	0.48	0.39	0.40	0.41	0.43	0.42	0.45	0.44
Fe3/(Fe3+Alvi)	0.59	0.00	0.00	0.00	0.00	0.00	0.64	0.68
Sum of S2	13.00	11.72	12.42	11.99	13.00	12.98	13.00	13.00
Amphibole names	magnesian hastingsitic hornblende	alumino-katophorite	subCa-Na-Al-ferro-edenite	K-subCa-Na-Al-Si ferro-edenite	ferroan pargasitic hornblende	ferroan pargasitic hornblende	potassian-magnesian hastingsitic hornblende	potassian-magnesian hastingsite
P (kbars)								
Hammarstrom & Zen 86	5.76	not valid*	11.23	not valid*	6.46	6.33	6.25	6.87
Hollister et al. 87	6.09		12.23		6.88	6.73	6.65	7.34
Johnson & Rutherford 89	4.68		9.28		5.27	5.16	5.09	5.62
Schmidt 92	6.15		11.33		6.81	6.69	6.62	7.20

(*)- Barometers are only valid for certain calcic amphiboles

Table 8. Representative amphibole microprobe analyses from the S-SBDZ brecciated metamafic rocks (locality 117). The program PROBE-AMPH (Tindle and Webb, 1994) was used to determine structural formula and mineral name.

Sample	117a2-3	117a2-6	117a2-8	117a2-10	117a2-11	117a2-21	117a2-25	117a2-36
Mineral	K-fsp	Plag	Plag	Plag	Plag	Plag	Plag	Plag
Na_2O	1.04	3.25	2.57	0.84	2.59	3.54	5.11	6.26
MgO	0.04	5.45	3	7.08	3.28	1.97	0.94	0.77
SiO_2	64.54	49.11	54.3	50.74	54.51	52.26	58.94	58.05
K_2O	16.1	2.89	6.64	1.62	5.27	0.64	3.71	1.37
TiO_2	0.49	0.59	0.52	0.55	1.04	8.49	0.87	0.09
MnO	0	0.2	0.16	0.31	0.25	0.11	0	0.23
FeO*	0.07	13.08	7.76	17.06	8.28	5.23	2.92	2.32
Al_2O_3	19.32	17.29	18.69	9.71	17.4	14.67	22.93	25.07
CaO	0	7.12	5.11	10.36	6.78	12.52	5.84	6.73
CalcTotal	101.6	99	98.75	98.26	99.4	99.44	101.24	100.9
OxNum	8	8	8	8	8	8	8	8
Si	2.94	2.43	2.62	2.58	2.62	2.49	2.66	2.61
Al	1.04	1.01	1.06	0.58	0.99	0.82	1.22	1.33
Fe*	0.00	0.54	0.31	0.73	0.33	0.21	0.11	0.09
Mg	0.00	0.40	0.22	0.54	0.24	0.14	0.06	0.05
Ca	0.00	0.38	0.27	0.56	0.35	0.64	0.28	0.32
Na	0.09	0.31	0.24	0.08	0.24	0.33	0.45	0.55
K	0.94	0.18	0.41	0.11	0.32	0.04	0.21	0.08
Ti	0.02	0.02	0.02	0.02	0.04	0.30	0.03	0.00
Mn	0.00	0.01	0.01	0.01	0.01	0.01	0.00	0.01
Albite	9	36	26	11	26	33	47	58
Anorthite	0	43	29	75	38	64	30	34
Orthoclase	91	21	45	14	35	4	23	8

Sample	117a2-39	117a2-40	117a2-42	117a2-43
Mineral	Biotite	Biotite	Biotite	Biotite
Na_2O	1.73	1.96	0.04	0.11
MgO	3.56	3.44	8.63	8.44
SiO_2	43.53	43.13	36.37	36.18
K_2O	1.59	1.57	3.46	3.52
TiO_2	2.64	2.83	2.38	2.37
MnO	0.08	0.16	0.16	0.16
FeO	8.2	8.08	16.31	16.04
Al_2O_3	20.23	20.11	17.8	17.84
CaO	15.45	15.38	9.06	9.33
CalcTotal	97.01	96.67	94.21	93.98
OxNum	22	22	22	22
Si	6.05	6.03	5.47	5.45
Al	3.32	3.31	3.15	3.17
Fe*	0.95	0.94	2.05	2.02
Mg	0.74	0.72	1.93	1.90
Ca	2.30	2.30	1.46	1.51
Na	0.47	0.53	0.01	0.03
K	0.28	0.28	0.66	0.68
Ti	0.28	0.30	0.27	0.27
Mn	0.01	0.02	0.02	0.02
#mg	43.62	43.16	48.53	48.41
Total Cat	14.39	14.43	15.03	15.05

Table 9. Representative microprobe analyses of feldspars and biotite from the fragments of the S-SBDZ brecciated metamafic rocks. The program MINTAB (Rock and Carroll, 1990) was used to determine structural formula.

Sample	117a3-8	117a3-14	117a3-17	117a3-22	Sample	117a3-25
Mineral	Plag	Plag	Plag	Plag	Mineral	Biotite
Na2O	6.77	11.02	10.58	6.29	Na2O	0.1
MgO	0	0	0	0.11	MgO	10.88
SiO2	59.76	69.56	69.33	60.69	SiO2	36.71
K2O	0.14	0.05	0.03	3.51	K2O	9.56
TiO2	0.05	0	0.01	0	TiO2	2.28
MnO	0	0	0	0.04	MnO	0.66
FeO*	0.2	0.16	0.2	0.2	FeO	21.53
Al2O3	27.03	20.64	20.86	27.79	Al2O3	16.63
CaO	8.02	0.28	0.56	2.51	CaO	0.09
CalcTotal	101.98	101.7	101.58	101.13	CalcTotal	98.43
OxNum	8	8	8	8	OxNum	22
Si	2.62	2.98	2.97	2.67	Si	5.48
Al	1.39	1.04	1.05	1.44	Al	2.93
Fe*	0.01	0.01	0.01	0.01	Fe*	2.69
Mg	0.00	0.00	0.00	0.01	Mg	2.42
Ca	0.38	0.01	0.03	0.12	Ca	0.01
Na	0.57	0.92	0.88	0.54	Na	0.03
K	0.01	0.00	0.00	0.20	K	1.82
Ti	0.00	0.00	0.00	0.00	Ti	0.26
Mn	0.00	0.00	0.00	0.00	Mn	0.08
mg	0.00	0.00	0.00	49.36	mg	47.38
Total Cat	4.98	4.96	4.94	4.98	Total Cat	15.72
Albite	60	98	97	63		
Anorthite	39	1	3	14		
Orthoclase	1	0	0	23		

Table 10. Representative microprobe analyses of minerals plagioclase and biotite from the matrix of the S-SBDZ brecciated metamafic rocks. The program MINTAB (Rock and Carroll, 1990) was used to determine structural formula.

Element in %	3	8	12	18	22	25	26	32	34
SiO_2	54.73	48.98	51.63	47.85	55.07	54.30	55.26	49.09	53.09
TiO_2	1.25	0.56	0.63	0.36	0.56	0.77	0.78	0.65	0.95
Al_2O_3	16.18	21.37	8.19	18.84	14.17	18.22	17.94	16.13	18.09
FeO*	10.34	7.00	11.60	7.30	8.37	8.69	8.45	9.26	9.74
MnO	0.22	0.12	0.24	0.12	0.14	0.13	0.13	0.17	0.13
MgO	2.83	4.66	11.20	8.14	7.01	4.42	3.75	7.55	3.61
CaO	4.86	11.70	13.27	13.60	7.61	7.12	6.30	10.87	7.15
Na_2O	4.22	2.49	1.25	1.55	2.70	3.18	3.44	2.45	3.75
K_2O	3.31	1.39	0.71	0.75	2.31	1.77	2.04	1.33	1.85
P_2O_5	0.63	0.13	0.22	0.07	0.28	0.30	0.28	0.20	0.30
LOI	0.59	1.75	1.03	1.63	1.54	1.04	1.22	1.82	1.29
Total	99.18	100.17	99.96	100.20	99.77	99.95	99.60	99.53	99.95
Element in ppm									
Ba	1322	359	217	232	586	652	745	1158	753
Co	33.4	37.8	59.1	42.8	51.1	44.9	44.3	51.5	44
Cs	1.4	2.1	0.8	3.4	2.6	2.5	3.6	2.7	3.8
Ga	25.4	19.4	15	16.1	18.1	21	23.8	17.7	23.6
Hf	8.6	1.4	2.2	0.8	3	2.8	3.6	2.2	2.9
Nb	24.5	2.5	3.5	1.2	7.5	6.2	7	4.1	7.1
Rb	98.1	39.2	22.9	29.1	92.6	55	84.8	49.2	64.3
Sn	2	1	2	0.5	2	2	3	2	2
Sr	384.3	740	329.1	827.8	534.6	938.2	756.1	488	939.4
Ta	1.4	0.2	0.4	0.1	0.8	0.5	0.6	0.3	0.7
Th	2.1	1.5	4.7	0.5	6.6	4.6	4.4	2.3	3.8
Tl	0.7	0.5	0.4	0.5	0.6	0.7	0.6	1.3	1.1
U	1.1	0.8	1.3	0.2	2.8	2.7	1.8	0.9	1.6
V	135	197	260	155	185	130	136	162	193
W	114	108	75	68	126	173	175	72	140
Zr	304.4	39.7	60.4	22.6	97.3	73.4	107.2	64.7	77.7
Y	47.4	10.7	22	6.9	21.1	18.3	23.5	17.6	20.7
La	61.3	12.2	33.9	5.7	34.8	25.9	27.8	18.1	27.8
Ce	128.2	23.2	79.2	12.3	78.5	51.4	57.8	37.7	57.2
Pr	15.91	2.97	10.87	1.65	9.98	6.63	7.29	4.74	7.08
Nd	65.4	12.7	50	7.5	43.6	26.3	29.5	20.9	29.8
Sm	12.1	2.7	11.2	1.7	8.5	5.1	5.8	4.3	6.1
Eu	3.19	0.99	3.12	0.76	2.38	1.69	1.69	1.36	1.81
Gd	8.13	2.51	7.78	1.72	6.08	4.36	4.83	4.14	4.68
Tb	1.33	0.33	0.88	0.24	0.76	0.72	0.7	0.56	0.65
Dy	8.24	1.76	4.6	1.37	4.31	3.61	4.15	3.35	3.82
Ho	1.63	0.36	0.75	0.24	0.73	0.87	0.84	0.63	0.75
Er	4.94	1.06	2.11	0.7	2.18	2.17	2.42	1.86	2.11
Tm	0.69	0.15	0.27	0.09	0.27	0.46	0.37	0.26	0.31
Yb	4.47	0.97	1.67	0.6	1.67	1.92	2.22	1.55	1.8
Lu	0.69	0.14	0.23	0.09	0.25	0.47	0.35	0.23	0.29
Mo	<1	1	<1	1	<1	<1	<1	<1	<1
Cu	45	58	117	59	56	78	19	164	119
Pb	3	4	<3	3	4	<3	3	7	<3
Zn	121	23	20	10	29	63	78	25	61
Ni	6	6	9	6	24	24	12	32	3
As	<2	<2	<2	<2	<2	<2	<2	<2	<2
Cd	<0.2	<0.2	<0.2	<0.2	<0.2	<0.2	<0.2	<0.2	<0.2
Sb	0.7	2.1	<0.5	1.1	<0.5	0.5	0.9	<0.5	<0.5
Bi	<0.5	<0.5	0.5	<0.5	<0.5	0.5	<0.5	<0.5	<0.5

Continuation on the next page

Element in %	35	38	39	40	41	117-2	117-3	117-4	117-5
SiO_2	49.94	47.45	45.04	44.69	46.30	49.91	59.61	51.31	65.04
TiO_2	0.89	0.73	0.19	1.70	1.25	1.03	0.66	0.83	0.55
Al_2O_3	17.33	16.32	18.59	18.17	17.35	16.66	17.95	14.43	15.75
FeO*	10.76	10.02	9.92	13.67	13.33	11.42	6.70	10.55	4.51
MnO	0.16	0.16	0.14	0.14	0.19	0.18	0.11	0.17	0.08
MgO	5.67	8.16	12.38	5.79	5.38	4.95	1.91	7.29	1.64
CaO	9.25	13.20	11.29	10.31	9.49	8.63	4.58	9.18	3.72
Na_2O	3.11	1.85	1.39	2.70	2.80	3.46	4.03	2.52	3.03
K_2O	1.29	0.64	0.25	0.89	1.80	1.70	3.13	1.65	3.83
P_2O_5	0.21	0.10	0.04	0.16	0.42	0.29	0.36	0.24	0.16
LOI	1.33	1.30	1.48	1.30	1.27	1.07	0.86	1.29	1.00
Total	99.94	99.92	100.71	99.50	99.59	99.29	99.91	99.45	99.31
Element in ppm									
Ba	419	151	183	235	841	498	982	653	1183
Co	49.1	52	73.6	65.3	54.7	48.2	31.8	53.5	48.8
Cs	1.9	1.4	0.9	2.6	2.2	1	1.6	1.8	3.9
Ga	23.7	17.1	14.2	25.9	28.1	21.8	21.5	18.4	21.4
Hf	2.2	1.3	0.6	1.8	6.2	2.3	6.6	2.8	6
Nb	6.5	2.4	0.7	5.7	12.2	5.4	9.9	6.2	12.5
Rb	45.1	22.9	7.2	29.8	66.3	50.8	87.3	57.3	144.7
Sn	1	2	0.5	2	2	0.5	1	1	3
Sr	864.9	795.7	773.7	910.4	581.6	893.8	903.8	748.2	453.1
Ta	0.5	0.3	<0.1	0.4	0.7	0.4	0.8	0.6	1.1
Th	2.6	1.5	0.4	1.6	2	3.3	13.6	6.2	11.7
Tl	0.9	1.1	0.8	0.6	0.5	0.3	0.4	0.4	0.7
U	0.8	1	0.1	0.7	0.9	1.3	6.3	2.3	2.8
V	228	223	73	367	256	218	59	179	75
W	74	60	45	79	66	97	180	107	338
Zr	63.7	28.5	15	43.5	224	60.4	223.3	72.9	180.5
Y	21.2	11.1	4.4	28.6	38.4	18.2	22.9	19.5	33.1
La	23	8.8	4.3	14.9	42	21.9	47.4	22.7	63.2
Ce	49.4	19.8	8.5	36.7	95	44.9	89.8	47.6	122
Pr	6.48	2.77	1.07	5.44	12.33	5.86	10.32	6.25	14
Nd	26.8	11.9	4.7	27.1	49.3	25.7	38.9	25.6	50.3
Sm	5.5	2.9	1.1	7.1	10.1	5.2	7.1	5.5	9.5
Eu	1.7	1.02	0.59	2.14	2.46	1.72	1.62	1.48	1.71
Gd	4.85	2.76	1.09	7.04	8.07	4.62	4.89	4.74	6.47
Tb	0.66	0.35	0.14	0.96	1.22	0.6	0.72	0.63	1.03
Dy	3.88	2	0.88	5.48	7.08	3.36	4.3	3.67	6.39
Ho	0.74	0.36	0.16	1.03	1.39	0.63	0.84	0.71	1.23
Er	2.14	1.07	0.44	3.02	4.05	1.92	2.49	2.07	3.72
Tm	0.3	0.16	0.06	0.38	0.56	0.25	0.35	0.28	0.49
Yb	1.83	0.88	0.38	2.3	3.4	1.56	2.29	1.78	2.94
Lu	0.25	0.13	0.06	0.31	0.48	0.23	0.34	0.26	0.42
Mo	<1	<1	<1	1	<1	<1	<1	<1	<1
Cu	112	221	102	331	134	59	3	61	21
Pb	<3	3	<3	<3	3	3	7	3	6
Zn	46	26	14	52	68	45	72	34	63
Ni	18	31	144	39	16	16	1	32	7
As	<2	<2	<2	<2	<2	<2	<2	<2	<2
Cd	<0.2	<0.2	<0.2	<0.2	<0.2	<0.2	<0.2	<0.2	<0.2
Sb	<0.5	1.2	1.5	0.7	<0.5	<0.5	1.1	<0.5	<0.5
Bi	0.5	<0.5	<0.5	0.5	<0.5	<0.5	0.5	<0.5	<0.5

Continuation on the next page

Element in %	121	122	123	124	126	127	128	130	131
SiO_2	49.32	45.09	46.83	48.82	55.18	54.14	55.51	55.41	47.61
TiO_2	0.58	1.34	1.22	1.03	0.68	0.80	0.73	0.71	0.74
Al_2O_3	10.67	17.41	17.91	16.91	15.92	17.11	17.71	18.25	16.27
FeO*	8.53	14.62	12.70	11.75	8.46	9.61	8.21	7.93	10.79
MnO	0.16	0.23	0.18	0.17	0.15	0.14	0.13	0.16	0.15
MgO	10.97	5.73	5.70	5.49	5.26	5.27	4.17	3.49	8.05
CaO	15.85	9.35	9.12	9.74	6.98	7.11	6.73	6.97	12.65
Na_2O	1.51	3.04	2.51	2.69	2.92	2.77	3.39	4.46	1.81
K_2O	0.70	0.75	1.11	1.30	2.10	1.71	1.83	1.04	0.68
P_2O_5	0.09	0.37	0.33	0.29	0.31	0.24	0.30	0.35	0.10
LOI	1.42	1.41	1.49	1.09	1.62	1.17	1.14	1.10	1.33
Total	99.81	99.34	99.11	99.29	99.58	100.08	99.86	99.88	100.15
Element in ppm									
Ba	349	351	1048	467	631	577	579	721	241
Co	54.3	61.5	54	51.2	47.5	53.6	46.8	42.9	54.7
Cs	1.9	2.2	2.2	1	5.3	3.5	2.6	1.1	2.8
Ga	12.8	25.7	23.4	21.8	19.6	21.1	22.4	22.3	18.1
Hf	1.3	2	3.2	2.4	4.4	2.8	3.1	3.3	1.3
Nb	1.9	8.2	6.1	5.5	11.3	6.8	6.7	6.2	2.3
Rb	27.7	26.4	31.5	37	100.4	62.9	59.8	45.6	32.3
Sn	0.5	0.5	1	1	2	1	2	2	0.5
Sr	532.7	758.5	736.4	1236	639.4	822.6	831	709.3	838.9
Ta	0.2	0.4	0.4	0.4	1	0.8	0.6	0.6	0.2
Th	1.9	0.6	1.8	2.8	7.2	5.2	4.4	4	1.7
Tl	0.2	0.3	0.3	0.1	0.4	0.4	0.2	0.2	0.1
U	0.7	0.3	5.4	1	2.8	2.6	1.6	2.7	0.6
V	210	277	251	226	146	167	134	125	230
W	52	67	49	84	144	153	187	188	43
Zr	30.6	45.5	85.3	66.3	122.1	75.6	89.7	100	29.9
Y	15.4	39.2	27	20	24.6	20.5	20.8	22	12.6
La	10	28	23.1	22.7	41	23.2	26.2	25.7	10
Ce	22.5	67.7	53.1	49	86.9	49.6	54.3	52.2	22.1
Pr	3.21	9.74	7.23	6.47	11.06	6.23	6.91	6.71	3.04
Nd	15	45.2	31	26.7	44.9	25.5	27.6	27.5	13.8
Sm	3.9	10.1	7.2	6.1	8.7	5.3	5.7	5.7	3.3
Eu	1.19	2.96	2.33	1.87	2.33	1.39	1.59	1.5	1.06
Gd	3.66	8.36	6.05	4.9	5.86	4.55	4.52	4.63	3.13
Tb	0.51	1.21	0.85	0.69	0.82	0.64	0.66	0.65	0.42
Dy	2.85	7.16	4.99	3.85	4.74	3.73	3.78	3.86	2.31
Ho	0.56	1.4	0.98	0.73	0.92	0.74	0.74	0.76	0.46
Er	1.6	3.94	2.71	2.05	2.62	2.19	2.21	2.27	1.3
Tm	0.2	0.54	0.35	0.27	0.36	0.31	0.31	0.32	0.18
Yb	1.25	3.23	2.23	2.6	2.34	1.87	1.97	1.95	1.08
Lu	0.18	0.47	0.34	0.24	0.34	0.28	0.29	0.3	0.17
Mo	<1	<1	<1	<1	<1	<1	<1	<1	<1
Cu	202	95	153	142	63	92	59	49	239
Pb	3	<3	3	<3	6	3	5	4	<3
Zn	13	68	52	53	52	55	74	49	13
Ni	78	13	20	24	25	32	26	11	28
As	<2	<2	<2	<2	<2	<2	<2	<2	<2
Cd	<0.2	<0.2	<0.2	<0.2	<0.2	<0.2	<0.2	<0.2	<0.2
Sb	<0.5	<0.5	<0.5	<0.5	<0.5	1	0.7	<0.5	<0.5
Bi	<0.5	<0.5	<0.5	<0.5	0.5	<0.5	<0.5	<0.5	<0.5

Continuation on the next page

Element in %	133	134	135	136	137	138	139	140	142
SiO_2	54.29	54.58	53.67	51.75	53.48	56.63	50.72	51.40	52.23
TiO_2	0.73	0.84	0.86	0.82	0.81	0.75	0.68	0.93	1.04
Al_2O_3	17.67	17.02	18.62	16.76	16.08	17.46	7.47	17.31	18.14
FeO*	9.00	9.13	8.27	9.32	8.97	7.53	8.65	10.85	9.80
MnO	0.13	0.16	0.13	0.18	0.14	0.14	0.17	0.14	0.16
MgO	4.67	4.63	3.99	5.83	6.08	3.57	11.95	4.86	3.54
CaO	7.77	7.27	7.38	9.18	7.69	6.83	16.64	7.92	6.79
Na_2O	2.93	3.05	4.43	2.97	3.02	3.46	1.83	3.60	4.55
K_2O	1.60	2.01	1.37	1.66	1.58	2.14	0.55	1.43	1.63
P_2O_5	0.17	0.23	0.41	0.20	0.60	0.28	0.13	0.16	0.94
LOI	1.38	1.09	0.37	1.37	1.32	1.22	1.41	1.01	0.80
Total	100.31	100.01	99.48	100.04	99.77	100.02	100.91	99.60	99.61
Element in ppm									
Ba	704	623	991	603	735	681	179	564	592
Co	48.4	51.8	44.6	49.9	49.7	36.7	46.8	57	36.6
Cs	2.2	6.2	0.9	2.7	1.4	2.3	0.3	3.1	5.2
Ga	20	22.3	27.3	20.1	20.8	19.1	11.1	20.4	21
Hf	2	2.8	2.8	2.3	4.7	3	2.1	2.5	1.9
Nb	4.5	7.2	5.4	7.4	11.4	6.5	2.7	5.2	5.2
Rb	60.9	93.2	26.1	48.6	39.7	65	22.2	56.4	55.8
Sn	1	4	2	2	2	1	1	1	1
Sr	736.6	697.2	1324	695.1	848.5	829.1	163.7	809.2	1064.3
Ta	0.5	0.8	0.3	0.7	0.6	0.6	0.2	0.4	0.4
Th	4.7	4.1	1.6	2.6	3	5.3	0.9	3.4	3.3
Tl	0.3	0.4	0.1	0.1	0.5	0.6	0.7	0.5	0.6
U	2.3	3.2	0.7	2.8	1.5	2.5	0.4	1.2	1.3
V	195	169	155	176	143	165	233	355	128
W	172	169	115	143	138	174	78	121	102
Zr	54.1	82	88.2	63.8	193.4	100.3	68.2	84.1	66.1
Y	13.7	22.6	17	19.5	21.4	17.2	20.1	14.7	23.1
La	21.2	25	30.8	22.4	49.7	26.4	10.7	20.6	34.3
Ce	42.6	53.5	64.8	47.9	101.9	55.3	26.4	42.5	73.8
Pr	5.09	6.8	8.42	5.72	11.84	6.44	3.54	5.1	9.02
Nd	19.9	27.9	34.6	22.7	47.3	26	17.4	20.9	39.9
Sm	3.8	5.9	6.4	4.6	7.9	5	4.4	3.8	7.2
Eu	1.1	1.58	1.89	1.37	2.05	1.39	1.38	1.22	2.37
Gd	3.36	4.73	4.42	3.91	5.19	3.78	4.05	3.34	5.53
Tb	0.45	0.71	0.58	0.55	0.79	0.54	0.63	0.44	0.77
Dy	2.57	4.01	3.3	3.42	4.46	3.29	3.89	2.79	4.38
Ho	0.52	0.82	0.61	0.68	0.78	0.62	0.77	0.55	0.82
Er	1.47	2.36	1.74	2.1	2.38	1.92	2.27	1.68	2.45
Tm	0.2	0.32	0.23	0.33	0.28	0.26	0.29	0.22	0.29
Yb	1.26	2	1.42	2.06	1.92	1.77	1.94	1.53	1.95
Lu	0.19	0.27	0.2	0.33	0.25	0.25	0.27	0.22	0.26
Mo	<1	<1	<1	<1	<1	<1	<1	<1	2
Cu	108	46	62	54	88	62	658	99	14
Pb	3	3	<3	3	3	4	24	<3	3
Zn	51	79	47	55	66	79	17	47	72
Ni	19	20	14	25	54	8	64	37	<1
As	<2	<2	<2	<2	<2	<2	<2	<2	<2
Cd	<0.2	<0.2	<0.2	<0.2	0.2	<0.2	<0.2	<0.2	<0.2
Sb	0.8	0.6	<0.5	<0.5	0.8	0.6	<0.5	<0.5	<0.5
Bi	<0.5	<0.5	<0.5	<0.5	0.6	<0.5	<0.5	<0.5	<0.5

Table 11. Whole-rock chemical analyses of the studied rocks (major elements by XRF in wt % and trace elements by ICP/MS (except Cu, Pb, Zn, Ni by ICP/ES) in ppm).

Element (wt %)		SiO_2	Al_2O_3	CaO	FeO*	K_2O	MgO	Na_2O	P_2O_5	TiO_2
AR117_5 Granitoid	AR117_5	65.04	15.75	3.72	4.51	3.83	1.64	3.03	0.16	0.55
AR117_4 Mafic fragments	AR117_4	51.31	14.43	9.18	10.55	1.65	7.29	2.52	0.24	0.83
AR117_3 Matrix	AR117_3	59.61	17.95	4.58	6.70	3.13	1.91	4.03	0.36	0.66
Calculated40%granite60%mafic	Calculated	59.55	15.22	5.90	6.93	2.96	3.90	2.83	0.19	0.66

Element (ppm)		Ba	Co	Nb	Rb	Sr	V	Zr	Y
AR117_5 Granitoid	AR117_5	1183	48.8	12.5	144.7	466.8	75	180.5	33.1
AR117_4 Mafic fragments	AR117_4	653	53.5	6.2	57.3	1034.5	179	72.9	19.5
AR117_3 Matrix	AR117_3	982	31.8	9.9	87.3	1215	59	223.3	22.9
Calculated40%granite60%mafic	Calculated	971.00	50.70	9.98	110.00	694.00	117.00	137.00	27.70

Element (ppm)		La	Ce	Nd	Sm	Eu	Gd	Tb	Dy	Er	Yb	Lu
AR117_5 Granitoid	AR117_5	63.2	122	50.3	9.5	1.71	6.47	1.03	6.39	3.72	2.94	0.42
AR117_4 Mafic fragments	AR117_4	22.7	47.6	25.6	5.5	1.48	4.74	0.63	3.67	2.07	1.78	0.26
AR117_3 Matrix	AR117_3	47.4	89.8	38.9	7.1	1.62	4.89	0.72	4.3	2.49	2.29	0.34
Calculated40%granite60%mafic	Calculated	47.00	92.20	40.40	7.90	1.62	5.78	0.87	5.30	3.06	2.48	0.36

Table 12. Model of mixing between the mafic rock (117-4) and granitoid (117-5). The composition of the analysed intermediate matrix (117-3) correlates with the calculated values of the hybrid rock, formed due to mixing of 40% of granite and 60% of metamafic rock.

Tidigare skrifter i serien "Examensarbeten i Geologi vid Lunds Universitet":

88. Gunnemyr, Lisa, 1997: Spårämnesförsök i konstgjort infiltrerat vatten -en geologisk och hydrogeologisk studie av Strömsholmsåsen, Hallstahammar, Västmanland.
89. Antonsson, Christina, 1997: Inventering, hydrologisk klassificering samt bedömning av hydrogeologisk påverkan av våtmarksområden i samband med järnvägstunnelbyggnation genom Hallandsåsen, NV Skåne.
90. Nordborg, Fredrik, 1997: Granens markpåverkan -en studie av markkemi, jordmånsbildning och lermineralogi i gran-och lövskogsbestånd i södra Småland.
91. Dobos, Felicia, 1997: Pollen-stratigraphic position of the last Baltic Ice Lake drainage.
92. Nilsson, Johan, 1997: The Brennvinsfjorden Group of southern Botniahalvøya, Nordaustlandet, Svalbard -structure, stratigraphy and depositional environment.
93. Tagesson, Esbjörn, 1998: Hydrogeologisk studie av grundvattnets kloridhalter på östra Lister-landet, Blekinge.
94. Eriksson, Saskia, 1998: Morängenetiska undersökningar i klintar vid Greifswalder Boddens södra kust, NÖ Tyskland.
95. Lindgren, Johan, 1998: Early Campanian mosasaurs (Reptilia; Mosasauridae) from the Kristianstad Basin, southern Sweden.
96. Ahnesjö, Jonas, B., 1998: Lower Ordovician conodonts from Köpings klint, central Öland, and the feeding apparatuses of *Oistodus lanceolatus* Pander and *Acodus deltatus* Lindström.
97. Rehnström, Emma, 1998: Tectonic stratigraphy and structural geology of the Ålkatj-Tielma massif, northern Swedish Caledonides.
98. Modin, Anna-Karin, 1998: Distributionen av kadmium i moränmark kring St. Olof, SÖ Skåne.
99. Stockfors, Martin, 1998: High-resolution methods for study of carbonate rock: a tool for correlating the sedimentary record.
100. Zillén, Lovisa, 1998: Late Holocene dune activity at Sandhammaren, southern Sweden - chronology and the role of climate, vegetation, and human impact.
101. Bernhard, Maria, 1998: En paleoekologisk - paleohydrologisk undersökning av våtmarkskomplexet Rolands hav, Blekinge.
102. Carlemalm,Gunnar, 1999: En glacialgeologisk studie av morän och moränfyllda sprickor i underliggande sandursediment, Örsjö, Skåne.
103. Blomstrand, Malou, 1999: 1992-1998 Seismicity and Deformation at Mt. Eyjafjallajökull volcano,South Iceland.
104. Dahlqvist, Peter, 1999: A Lower Silurian (Llandoverian) halysitid fauna from the Berge Limestone Formation, Norderön, Jämtland, central Sweden.
105. Svensson, Magnus A., 1999: Phosphatized echinoderm remains from upper Lower Ordovician strata of northern Öland, Sweden - preservation, taxonomy and evolution.
106. Bengtsson, Anders, 1999: Trilobites and bradoriid arthropods from the Middle and Upper Cambrian at Gudhem in Västergötland, Sweden.
107. Persson, Christian, 1999: Silurian graptolites from Bohemia, Czech Republic.
108. Jacobson, Mattias, 1999: Five new cephalopod species from the Silurian of Gotland.
109. Augustsson, Carita, 1999: Lapillituff som bevis för underjurassisk vulkanism av strombolikaraktär i Skåne.
110. Jensen, Sigfinn J., 1999: En silurisk transgressiv karbonatlagerföljd vid S:t Olofsholms stenbrott, Gotland.
111. Lund, Mats G., 1999: En strukturgeologisk modell för berggrunden i Sarvesvagge - Luottalako-området, Sareks Nationalpark, Lappland.
112. Magnusson, Jakob, 1999: Exploration of submarine fans along the Coffee Soil Fault in the Danish Central Graben.
113. Wickström, Jenny, 1999: Conodont biostratigraphy in Volkhovian sediments from the Mäekalda section, north-central Estonia.
114. Sjögren, Per, 1999: Utmarkens vegetationsutveckling vid Ire i Blekinge, från forntid till nutid -en pollenanalytisk studie.
115. Sälgeback, Jenny, 1999: Trace fossils from the Permian of western Dronning Maud Land, Antarctica.
116. Söderlund, Pia, 1999: Från gabbro till granatamfibolit. En studie av metamorfos i Åker-metabasiten väster om Protoginzonen, Småland.
117. Jönsson, Karl-Magnus, 2000: Sedimentologiska och litostratigrafiska undersökningar i södra Malmös kvartära avlagringar, södra Sverige.
118. Romberg, Ewa, 2000: En sediment-och biostratigrafisk undersökning av den tidigare Littorina-lagunen vid Barsebäck, SV Skåne, med beskrivning av en Preboreal klimatoscillation.
119. Bergman, Jonas, 2000: Skogshistoria i Söderåsens nationalpark. En pollenanalytisk studie i Söderåsens nationalpark, Skåne.
120. Lindahl, Anna, 2000: En paleoekologisk och paleohydrologisk studie av fuktängar i Bräkneåns dalgång, Bräkne-Hoby, Blekinge.

121. Eneroth, Erik, 2000: En paleomagnetisk detaljstudie av Sarekgångsvärmen.
122. Terfelt, Fredrik, 2000: Upper Cambrian trilobite faunas and biostratigraphy at Kakeled on Kinnekulle, Västergötland, Sweden.
123. Sundberg, Sven Birger, 2000: Vattenrening genom komplexbildning mellan järn och humusämnen -en litteraturstudie med försök.
124. Sundberg, Sven Birger, 2000: Sedimentationsprocesser och avlagringsmiljö för en kantrygg kring platåleran vid Rydsgårds gods i backlandskapet söder om Romeleåsen, Skåne.
125. Kjöllerström, Anders, 2000: En geokemisk studie av bergartsvariationen på Bullberget i västra Dalarna.
126. Cinthio, Kajsa, 2000: Senglacial och tidigholocen etablering och expansion av lövträd på en lokal i nordvästra Rumänien.
127. Lamme, Sara, 2000: Klimat-och miljöförändringar under holocen i Sylarnaområdet, södra svenska Skanderna, baserat på analys av makrofossil och klyvöppningar.
128. Jönsson, Charlotte, 2000: Geologisk och hydrogeologisk modellering av området mellan Bjuv och Söderåsen, nordvästra Skåne.
129. Kleman, Johan, 2001: Utvärdering av den underkambriska litostratigrafin på Österlen, södra Sverige.
130. Sundler, Malin, 2001: En jämförande studie mellan uppmätt och MACRO-simulerad pesticidutlakning på ett odlingsfält i Skåne.
131. Grönholm, Anna, 2001: Högtrycksmetabasiter i den södra delen av Mylonitzonen: fältgeologi, petrografi och metamorf utveckling.
132. Ekdahl, Magnus, 2001: En studie av Källsjögranitens deformationsmönster och kinematiska indikatorer inom Ullaredszonen.
133. Axheimer, Niklas, 2001: Middle Cambrian trilobites and biostratigraphy of the Almbacken drill core, Scania, Sweden.
134. Lindén, Mattias, 2001: Proglacial deformation of glaciofluvial sediments during the Pomeranian deglaciation in the Neubrandenburg area, NE Germany.
135. Warnhag, Jon, 2001: A geochemical study of the zoned Pan-African Mon Repos intrusion, Central Namibia.
136. Lundmark, Mattias, 2001: Zirkonstudie av Norra Hortens bergarter, SV Sverige.
137. Gunnarson, Rebecka, 2001: Sedimentologisk undersökning av en moränskärning i en djupvittrad sprickdal på Romeleåsen, Skåne.
138. Karlsson, Christine, 2001: Diagenetic and petrophysical properties of deeply versus moderately buried Cambrian sandstones of the Caledonian foreland, southern Sweden.
139. Eriksson, Mårten, 2001: Bedömning av föroreningsspridning kring en nedlagd bensinstation i Karlaby, sydöstra Skåne.
140. Ljung, Karl, 2001: Apaleoecological study of the Pleistocene-Holocene transition in the Kap Farvel area, South Greenland.
141. Åkesson, Cecilia, 2001: Undersökning av grundvattenförhållanden i området kring Östra Vemmerlöv, Simrishamns kommun, sydöstra Skåne.
142. Bermin, Jonas, 2001: Modelling Mössbauer spectra of biotite.
143. Mansurbeg, Howri, 2001: Modelling of reservoir quality in quartz-rich sandstones of the Lower Cretaceous Bentheim sandstones, Lower Saxony Basin, NW Germany.
144. Hermansson, Tobias, 2001: Sierggavággeskollans strukturgeologiska utveckling; nyckeln till Sareks berggrundsgeologi.
145. Veres, Daniel-Stefan, 2001: A comparative study between loss on ignition and total carbon analysis on Late Glacial sediments from Atteköps mosse, southwestern Sweden, and their tentative correlation with the GRIP event stratigraphy.
146. Ahlberg, Tomas, 2001: Hydrogeologisk undersökning samt sårbarhetskartering av området kring tre bergborrade grundvattenanläggningar i Simrishamns kommun.
147. Boman, Daniel, 2001: Tektonostratigrafi och deformationsrelaterad metamorfos i norra Kebnekaisefjällen, Skandinaviska Kaledoniderna.
148. Olsson, Stefan, 2002: The geology of the Portobello Peninsula; proposal of a saturated to oversaturated lineage within the Dunedin Volcano, New Zealand.
149. Molnos, Imre, 2002: Petrografi och diagenes i den underkambriska lagerföljden i Skrylle, Skåne.
150. Malmborg, Pär, 2002: Correlation between diagenesis and sedimentary facies of the Bentheim Sandstone, the Schoonebeek field, The Netherlands.
151. Jonsson, Henrik, 2002: Permeability variation in a tidal Jurassic deposit, Höganäs basin, Fennoscandian Border Zone
152. Lundgren, Anders, 2002: Seveskollorna i nordöstra Kebnekaise, Kaledoniderna: metabasiter, graniter och ögongnejser.
153. Sultan, Lina, 2002: Reconstruction of fan-shaped outwash in front of the Mýrdalsjökull ice cap, Iceland: Architecture and style of sedimentation.
154. Rimša, Andrius, 2002: Petrological study of the metamafic rocks across the Småland-Blekinge Deformation Zone